TROPOMI-derived NO2 emissions from copper/cobalt mining and other industrial activities in the Copperbelt (DRC and Zambia)

Sara Martinez-Alonso[1], Pepijn Veefkind[2], Barbara Klara Dix[3], Benjamin Gaubert[4], Nicolas Theys[5], Claire Granier[6], Antonin Soulié[7], Sabine Darras[8], Henk Eskes[2], Wenfu Tang[9], Helen M. Worden[1], Joost A de Gouw[3], and Pieternel F Levelt[10]

[1]National Center for Atmospheric Research (UCAR)
[2]Royal Netherlands Meteorological Institute
[3]University of Colorado Boulder
[4]National Center for Atmospheric Research (NCAR)
[5]Belgian Institute for Space Aeronomy (BIRA-IASB)
[6]NOAA Aeronomy Laboratory
[7]Université de Toulouse
[8]Observatoire Midi-Pyrenees
[9]NCAR
[10]National Center for Atmospheric Research

April 30, 2023

Abstract

We have analyzed TROPOMI data over the Copperbelt mining region (Democratic Republic of Congo and Zambia). Despite high background values, we find that annual 2019-2022 means of TROPOMI NO2 show local enhancements consistent with six point sources (mines and cities) where high-emission industrial activities take place. We have quantified annual NO2 emissions for the six sources, identified temporal trends in these emissions, and found strong correlations with mine/refinery production data. CAMS-GLOB-ANT v5 inventory emissions are lower than TROPOMI-derived emissions by 61-96 % and lack the temporal trends observed in TROPOMI and mine/oil refinery production. Lack of TROPOMI SO2 enhancements over the point sources analyzed indicates SO2 capture and transformation into sulfuric acid, a profitable byproduct. These results demonstrate the potential for satellite monitoring of mining/oil refining activity which impacts the air quality of local communities. This is particularly important for Africa, where mining is increasing aggressively.

TROPOMI-derived NO_2 emissions from copper/cobalt mining and other industrial activities in the Copperbelt (DRC and Zambia)

S. Martínez-Alonso[1], J. P. Veefkind[2,3], B. Dix[4], B. Gaubert[1], N. Theys[5], C. Granier[4,6,7], A. Soulié[6], S. Darras[8], H. Eskes[2], W. Tang[1], H. Worden[1], J. de Gouw[4,9], and P. F. Levelt[1,2,3]

[1]ACOM-NCAR, Boulder, Colorado, USA
[2]KNMI, De Bilt, The Netherlands
[3]Department of Civil Engineering and Geosciences, Technical University of Delft, Delft, The Netherlands
[4]CIRES, University of Colorado, Boulder, Colorado, USA
[5]BIRA-IASB, Brussels, Belgium
[6]Laboratoire dA´erologie, CNRS, University of Toulouse UPS, Toulouse, France
[7]NOAA-CSL, Boulder, Colorado, USA
[8]Observatoire Midi-Pyr´en´ees, Toulouse, France
[9]Department of Chemistry, University of Colorado Boulder, Boulder, Colorado, USA

Key Points:

- We quantified annual 2019-2022 TROPOMI-derived NO_2 emissions from six point sources in the Copperbelt, despite high background emissions.
- Annual TROPOMI-derived NO_2 emissions from these point sources are strongly correlated with annual mine/oil refinery production.
- Lack of elevated SO_2 at these point sources is consistent with SO_2 capture and production of sulfuric acid, a profitable byproduct.

Corresponding author: Sara Martínez-Alonso, sma@ucar.edu

Abstract

We have analyzed TROPOMI data over the Copperbelt mining region (Democratic Republic of Congo and Zambia). Despite high background values, we find that annual 2019-2022 means of TROPOMI NO_2 show local enhancements consistent with six point sources (mines and cities) where high-emission industrial activities take place. We have quantified annual NO_2 emissions for the six sources, identified temporal trends in these emissions, and found strong correlations with mine/refinery production data. CAMS-GLOB-ANT v5 inventory emissions are lower than TROPOMI-derived emissions by 61-96 % and lack the temporal trends observed in TROPOMI and mine/oil refinery production. Lack of TROPOMI SO_2 enhancements over the point sources analyzed indicates SO_2 capture and transformation into sulfuric acid, a profitable byproduct. These results demonstrate the potential for satellite monitoring of mining/oil refining activity which impacts the air quality of local communities. This is particularly important for Africa, where mining is increasing aggressively.

Plain Language Summary

We show that air pollution from copper/cobalt mines and oil refineries can be identified and measured from satellite, even in the presence of high background pollution from biomass burning and other sources; our findings may apply as well to other industries that consume large quantities of fossil fuels. This is important for monitoring the air quality of local communities, particularly when these industrial activities take place in close proximity to population centers, as is the case in the Copperbelt and, in general, in other African regions where mining and related industrial activities proliferate without sufficient air quality monitoring. Additionally, we show for the first time that the amount of air pollution measured by TROPOMI is strongly correlated with mine/refinery production. Studies like this can be used to estimate mine/refinery production before companies release their annual reports or (as is the case with non-publicly traded companies) in the absence of such reports. Insufficient emissions from mines claiming high production may be indicative of production from a different source. Thus, this method may help improve the traceability of minerals extracted in conflict areas and smuggled into the global supply chain despite existing traceability and tagging schemes.

1 Introduction

The Copperbelt, a mining region straddling the DRC (Democratic Republic of Congo) and Zambia, is currently of great strategic interest because it is the world's largest cobalt producer and holds almost half of the world reserves (Shedd, 2022). Cobalt production in the Copperbelt (mostly in the DRC) has increased $\sim$600% between 1990 and 2021 (U.S. Bureau of Mines, 1993; Shedd, 2022), driven by its use in lithium-ion batteries which power mobile phones, laptops, and electric cars. Access to the Copperbelt's cobalt is becoming a matter of national and global energy security (Gulley, 2022). Cobalt is, however, a byproduct of copper mining; copper is the main ore (by volume) extracted in the Copperbelt. Previous studies have documented the impact of cobalt and/or copper mining in the region's soils and water (Atibu et al., 2016), land use (Mwitwa et al., 2012), and neonatal health (Kayembe-Kitenge et al., 2019; Van Brusselen et al., 2020). The impact on local air quality remained unknown. Here we quantify the effect of increasing mining activity on the air quality of this region using TROPOMI (TROPOspheric Monitoring Instrument) satellite measurements (Veefkind et al., 2012) of NO_2 (nitrogen dioxide); TROPOMI SO_2 (sulfur dioxide) is also analyzed. Both gases are atmospheric pollutants (World Health Organization, 2021) relevant to air quality monitoring and forecasting. They are also considered short-lived climate forcers, important for understanding climate (Myhre et al., 2013).

NO_x (NO_2 + NO, two species closely intertwined by oxidation and reduction reactions), has both anthropogenic (fossil fuel combustion, biomass burning) and natural (microbial activity in soils, lightning, wildfires) sources. Mining-related NO_x is produced by high-temperature combustion of fuel used by trucks and other heavy machinery as well as by electric generators. The main sink of NO_x is the hydroxyl radical (OH), with which it reacts within hours in the presence of light. NO_x has a negative impact on air quality, both directly and as a precursor to tropospheric ozone and particulate matter. It is damaging to human health (affecting mostly the respiratory system) and crops, and contributes to the formation of smog and acid rain. Hereafter we discuss NO_2, the NO_x component measurable from satellite.

Measuring global and regional NO_2 was made possible by satellite instruments such as GOME (Global Ozone Monitoring Experiment), SCIAMACHY (SCanning Imaging Absorption SpectroMeter for Atmospheric CHartographY), OMI (Ozone Monitoring Instrument), and GOME-2, (Leue et al., 2001; Richter et al., 2005; Beirle et al., 2011; Richter et al., 2011). Labzovskii et al. (2022) reported regional-scale correlation between OMI NO_2 column values from heavy industry, including mining, and a coal production interannual variability index for the Siberian Kuzbass Basin. Thanks to its higher spatial resolution, TROPOMI allows for the measurement of NO_2 over smaller domains such as gas and oil fields (Dix et al., 2022), cities (Goldberg et al., 2019; Pommier, 2022; de Foy & Schauer, 2022), and power plants (Beirle et al., 2019, 2021; Goldberg et al., 2019; Dix et al., 2022; de Foy & Schauer, 2022).

SO_2 results from both anthropogenic (e.g., coal combustion, smelting of sulfur-rich ores) and natural (volcanism, marine biological processes) sources. It contributes to acid rain and particle formation. Exposure to SO_2 is harmful to human health, damages foliage, and impedes plant growth. Previous studies showed that SO_2 emissions could be estimated using satellite data from TOMS (Total Ozone Mapping Spectrometer), GOME, OMI, SCIAMACHY, and OMPS (Ozone Mapping and Profiler Suite) (Krueger, 1983; Carn et al., 2007; V. E. Fioletov et al., 2013; Zhang et al., 2017). V. Fioletov et al. (2020, 2023) reported TROPOMI-based emission estimates of SO_2 from power plants, volcanoes, oil and gas fields, and smelters.

We show that copper/cobalt mining-related activities, among others, can be identified and their NO_2 emissions quantified based on TROPOMI data even in the presence of high background values from biomass burning and other sources (BIRA-IASB, 2021). Additionally, we identify inter-annual trends in TROPOMI-derived NO_2 emissions that are strongly correlated with mining and oil refinery production. Next we describe the datasets (Sect. 2) and methodology (Sect. 3) used in this study, we present our results (Sect. 4), and discuss their relevance (Sect. 5). Conclusions are offered in Sect. 6.

2 Datasets

TROPOMI, onboard the European Space Agency's Sentinel-5 Precursor satellite (Veefkind et al., 2012), provides quasi-global daily coverage at high spatial resolution (3.5 x 5.5 km^2 for our species of interest). This is a nadir-viewing imaging spectrometer in a sun-synchronous orbit at 824 km of altitude, with 13:30 LST Equator-crossing time, and 2600 km swath width. TROPOMI measures radiances in the ultraviolet, visible, and reflected infrared, from which concentrations of trace gases as well as cloud and aerosol properties are derived. Here we focus on TROPOMI measurements of tropospheric NO_2 and SO_2, two pollutants produced by mining-related activities. NO_2 is retrieved from TROPOMI radiance measurements in the visible portion of the spectrum (400-496 nm) (van Geffen et al., 2020; H. J. Eskes & Eichmann, 2021; H. Eskes et al., 2022). We used daily TROPOMI NO_2 tropospheric column data from version 2 for the period between 1 January 2019 and 31 December 2022. We also analyzed TROPOMI SO_2 data retrieved with the Covariance-Based Retrieval Algorithm (COBRA, Theys et al. (2021)) from ultraviolet-visible radiances (310.5-326 nm) (Theys, 2022) for the 1 January 2019 - 31 July 2022 period; more recent data were unavailable at the time of writing.

Meteorological information needed to derive emissions from TROPOMI NO_2 VCD (vertical column density) was obtained from reanalysis data. By combining measurements and model results, reanalyses datasets provide consistent and gapless global coverage of essential climate variables. We used hourly ERA5 (ECMWF Reanalysis v5) data (Hersbach et al., 2020) provided at 0.25° x 0.25° resolution and generated by the Copernicus Climate Change Service at the European Center for Medium-Range Weather Forecasts.

Due to the unavailability of ground measurements, we compared inventory data to TROPOMI-derived NO2 emissions. Emission inventories are compilations of amounts of air pollutants released into the atmosphere, segregated by source and time period. We used 2019-2021 data from the CAMS-GLOB-ANT (Copernicus Atmosphere Monitoring Service Global Anthropogenic) emissions inventory version 5, an extension of version 4.2 (Granier et al., 2019). Inventory emissions for 2022 were unavailable at the time of writing. We focused on monthly NOx emissions, provided at 0.1° x 0.1° resolution.

Mine production data were obtained from the annual reports of publicly traded mining companies; these reports are mandated by official regulatory bodies such as the Securities and Exchange Commission in the United States and the Securities and Futures Commission in Hong Kong. Private mining companies are not required to disclose their production data. The specifics of the information available in these reports varies greatly.

3 Methodology

To identify potential emission point sources such as mines, we produced annual means from daily TROPOMI NO_2 VCD for the Copperbelt study area (-10.5°N to -13.5°N, 24.5°E to 29.5°E). Temporal averaging enhances the signal from constantly emitting sources while dampening more sporadic, background emissions from biomass burning, soils, and lightning.

Once the point sources were identified, we calculated daily TROPOMI-derived NO_2 emissions for the study area using the divergence method (Beirle et al., 2019; Dix et al., 2022) with some modifications described below. This method derives emission based on a divergence term and a sink term, which account for wind dispersion effects and NO_2 depletion by OH, respectively. A detailed description of the derivation can be found in Dix et al. (2022). To calculate daily emissions we regridded daily VCD values to a common 0.025° x 0.025° grid. We filtered TROPOMI measurements to avoid clouds, errors, and problematic retrievals by using only those with quality assurance value ≥ 0.75 (H. Eskes et al., 2022); retrievals with solar zenith angle $> 60°$ were rejected. Hourly values of fields (longitudinal and latitudinal horizontal wind at 100 m from the ground, pressure, and temperature) required for the emissions calculation were obtained from ERA5 reanalysis. All ERA5 fields were resampled to 0.025° x 0.025° spatial resolution and interpolated to the passing time of the closest (spatially and temporally) TROPOMI observation. Fields provided on pressure levels were interpolated to an altitude of 100 m above the ground. In our implementation, OH lifetime was calculated for each data point based on the solar zenith angle of the closest TROPOMI retrieval. Daily emissions were averaged into annual means.

To calculate the actual NO_2 emissions released from each point source, background NO_2 emissions must be quantified and removed from the raw (non-background corrected) emissions. Several background removal approaches are possible: Beirle et al. (2019) subtracted from the emissions their 10th percentile value, Dix et al. (2022) removed the mode of a Gaussian curve fit to them. We find that the former is better suited to study regions with homogeneous background emissions and that results from the latter are highly dependent on how the Gaussian curve is defined. Similarly, statistics derived from two-dimensional

Gaussians fitted to the point source emissions (Beirle et al., 2019) were, in our case, highly dependent on location and size of the area selected to perform the fit. Our approach consisted of calculating annual statistics (mean and standard deviation) for each point source plume as well as for its local background area: a $\sim 1^o$ x 1^o region surrounding each point source, excluding the point source plume. The location and extent of the point source plumes were identified based on an empirical threshold (0.37 kg km^{-2} h^{-1}) applied to mean raw emissions from the 2019-2022 period. Annual means of background-removed emissions were calculated for each point source by subtracting its mean background value from its mean raw emission value.

Dix et al. (2022) described in detail the effects of individual parameters (e.g., background correction, wind level, wind data source, OH lifetime, VCD thickness) on the results obtained using this method. We investigated ERA5 wind data uncertainty effects by using the spread of its wind field 10 member ensemble to perturb 2020 NO_2 emissions. The spread provides an estimate of relative, random uncertainty; ensemble, mean, and spread are part of the ERA5 dataset. The results show that ERA5 wind uncertainty produces small changes in raw NO_2 emission (< 4 %; Table S1 and Fig. S1).

4 Results

Six distinct point sources are clearly visible in the mean 2019-2022 TROPOMI NO_2 VCD map (Fig. 1; Fig. S2 shows annual mean VCD maps). Four of the point sources correspond to large copper (Sentinel, a.k.a. Trident; Lubumbashi; Kansanshi) or copper-cobalt (Kolwezi and adjacent Katanga) open-pit mines. The remaining two point sources coincide with cities (Lubumbashi and Ndola) where we infer that high-emission industrial activities take place, as explained below. Latitudinal profiles of mean annual VCD across each point source (Fig. 1) show that background NO_2 remains nearly constant year to year while the point sources (well defined, narrow peaks of fixed location) vary in magnitude. TROPOMI emission results (Table 1 and Fig. S3) reinforce these observations. TROPOMI NO_2 mostly increased with time at all the point sources but one, Ndola, where background-removed emissions decreased by > 70 % between 2019 and 2022.

To understand these inter-annual trends in NO_2 emissions, we compared background-removed TROPOMI-derived emissions to mine production data where available (Table 1 and Fig. 2). Most of the energy consumed in copper or copper-cobalt mining, including electricity, is generated by diesel fuel combustion. Mining equipment consumes $\sim$60 % of the total energy; comminution $\sim$36 %; flotation, filtering, and drying $\sim$4 % (Allen, 2021). Limited data relevant to energy consumption is provided in mining company reports; we found the best proxy for energy (i.e., diesel) consumed to be amount of ore and waste mined. Panels b, c, and d in Fig. 2 show strong positive correlation between annual values of total ore plus waste mined versus NO_2 emissions for the Sentinel, Lumwana, and Kansanshi mines (R = 0.84, 0.74, and 0.79, respectively). Amount of copper produced (highly dependent on ore grade, among other factors, and thus, a less-desirable proxy) was used for the Kolwezi-Katanga mines (Fig. 2.a) for lack of ore and waste data ($R = 0.84$).

The remaining two point sources coincide with some of the largest cities in the study area: Lubumbashi (DRC, population > 2.6 x 10^6) and Ndola (Zambia, population > 0.5 x 10^6). To discard the hypothesis that their emissions are due to urban activity alone, we quantified NO_2 emissions for two additional cities of similar size: Mbuji-Mayi (DRC, population > 2.7 x 10^6), located 750 km northwest of Lubumbashi; and Kitwe (Zambia, population > 0.7 x 10^6), 50 km northwest of Ndola (labeled g in Fig. 1 map). (Population data are for 2022 urban areas (Population Stat, 2023).) The results (Fig. 1, Table S2, and Fig. S4) show that neither the magnitude of VCD or emissions, the spatial extent of the plumes, or the temporal emission trends from Lubumbashi and Ndola can be explained by urban activity alone. Background-removed NO_2 emissions from Lubum-

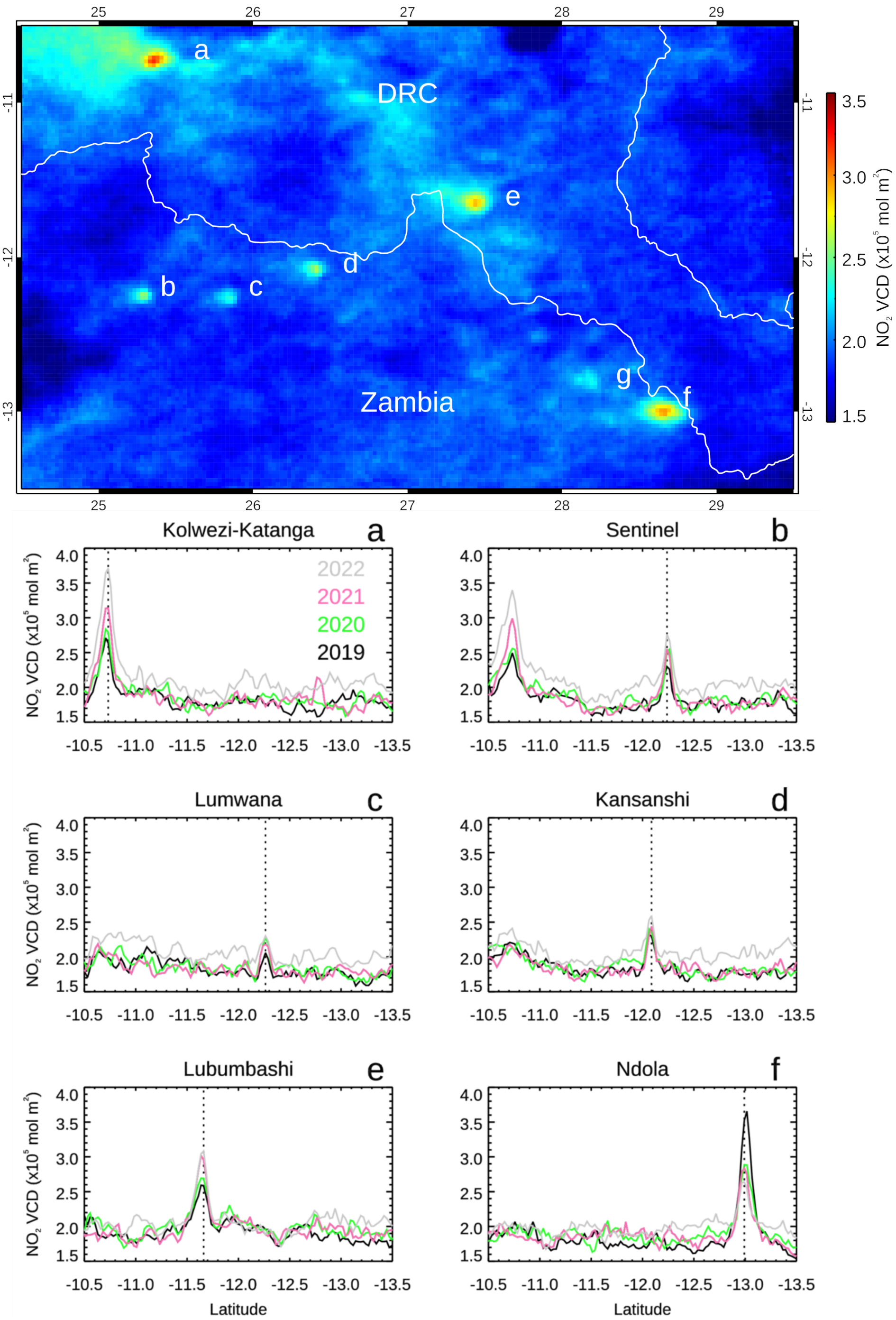

Figure 1. (Top) 2019-2022 mean of TROPOMI NO_2 VCD for the Copperbelt study region. Labels a through f show the six point sources analyzed. Label g shows the location of Kitwe City. White lines indicate country borders. (Bottom) Annual means of TROPOMI NO_2 VCD along latitudinal profiles centered at each of the six point sources, shown by vertical dotted lines. Labels as above. Profiles are color-coded according to year.

Table 1. Production and NO_2 emissions (TROPOMI background-removed, TROPOMI background, inventory) for six Copperbelt point sources. Ore, waste, and copper produced are in ktonnes; copper grade in percentage. Kansanshi reports provide separate copper grade values for sulfide, mixed, and oxide ores. Throughput (slag processed in Lubumbashi, crude refined in Ndola) are in ktonnes. All emissions and their standard deviation values (in parenthesis) are in kg km^2 h^{-1}.

		2019	2020	2021	2022
	Ore, Waste	-, -	-, -	-, -	-, -
	Grade	4.2, -	4.17, -	2.9, -	-, -
	Copper	84.3, 234.5	114.3, 270.7	121.1, 264.4	-, 220.1
Kolwezi[a], Katanga[b]	TROPOMI	0.19 (0.10)	0.24 (0.12)	0.31 (0.15)	0.41 (0.17)
	Background	0.23 (0.08)	0.23 (0.10)	0.22 (0.10)	0.26 (0.10)
	Inventory	0.03	0.03	0.03	-
	Ore, Waste	50263, 92826	60098, 97970	57380, 102445	56219, 95335
	Grade	0.5	0.49	0.47	0.46
	Copper	220.006	251.216	232.688	242.451
Sentinel[c]	TROPOMI	0.23 (0.11)	0.27 (0.12)	0.33 (0.10)	0.26 (0.11)
	Background	0.20 (0.07)	0.22 (0.08)	0.21 (0.07)	0.24 (0.07)
	Inventory	0.01	0.01	0.01	-
	Ore, Waste	23230, 62837	26880, 73480	33510, 65499	20277, 78063
	Grade	0.47	0.52	0.46	0.52
	Copper	107.955	125.191	109.769	121.109
Lumwana[d]	TROPOMI	0.20 (0.06)	0.29 (0.08)	0.27 (0.09)	0.21 (0.06)
	Background	0.21 (0.07)	0.22 (0.07)	0.21 (0.07)	0.24 (0.07)
	Inventory	0.04	0.04	0.04	-
	Ore, Waste	36325, 52768	34423, 61972	35142, 69758	28205, 75878
	Grade	0.89, 1.05, 1.12	0.83, 1.00, 0.93	0.88, 0.96, 0.72	0.71, 0.63, 0.57
	Copper	232.243	221.487	202.159	146.282
Kansanshi[c]	TROPOMI	0.22 (0.07)	0.31 (0.09)	0.33 (0.11)	0.28 (0.10)
	Background	0.22 (0.07)	0.23 (0.08)	0.22 (0.07)	0.24 (0.07)
	Inventory	0.08	0.08	0.08	-
	Throughput	-	-	255.229	-
Lubumbashi[e]	TROPOMI	0.23 (0.10)	0.23 (0.10)	0.30 (0.16)	0.28 (0.17)
	Background	0.25 (0.08)	0.26 (0.08)	0.25 (0.08)	0.26 (0.08)
	Inventory	0.25	0.26	0.26	-
	Throughput	700.277	372.384	56.672	0[g]
Ndola[f]	TROPOMI	0.58 (0.30)	0.32 (0.10)	0.26 (0.13)	0.17 (0.10)
	Background	0.20 (0.09)	0.21 (0.09)	0.21 (0.08)	0.23 (0.08)
	Inventory	0.22	0.22	0.22	-

[a]Zijin (2023). [b]Glencore (2023). [c]First Quantum (2023a). [d]Barrick (2023). [e]STL (2023). [f]Mwila et al. (2022). [g]Inactive.

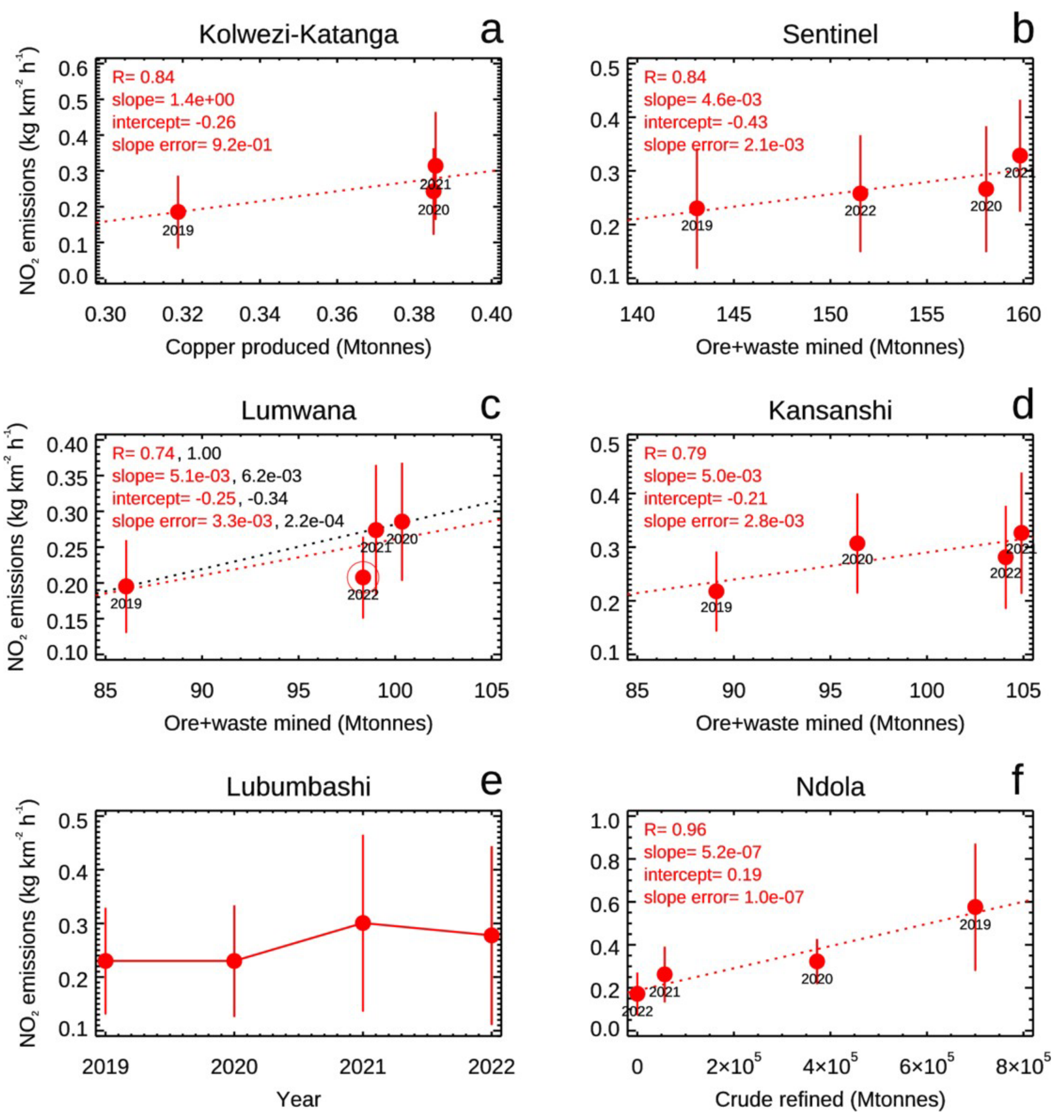

Figure 2. TROPOMI-derived, background-removed NO_2 emissions and their standard deviation versus production, except (e), where production data is unavailable. (c) Statistical values and fit line in black exclude 2022 values; see text for details.

bashi are higher than those from Mbuji-Mayi by 90 %, even though the population of the former is lower by 2 %. Similarly, while its population is lower by 27 %, emissions from Ndola surpass those from Kitwe by 40-80 %, depending on the year, and display inter-annual variations which do not correlate with changes in population. These findings are consistent with our hypothesis that emissions from Lubumbashi and Ndola are not the result of urban activity alone. We researched other possible origins for the excess emissions observed at these two point sources. We hypothesize that Lubumbashi's high NO_2 emissions are due to reprocessing of the Lubumbashi slag heap: a 14.5×10^6 tonne hill of mining residue located inside the city, resulting from metallurgical activity between 1924 and 1992 (Peˇsa, 2022). Copper, cobalt, and zinc are extracted from the slag heap by La Société Congolaise du Terril de Lubumbashi (2000-present). Reports from the local press attest to the pollution resulting from the operation (Africa Intelligence, 2021). Figure 2.e shows annual background-removed TROPOMI-derived NO_2 emissions; because production data is incomplete (STL, 2023; The Carter Center, 2023), emissions and mining-related activity cannot be compared in this case. The most plausible emissions source in Ndola is the INDENI petroleum refinery plant, located inside the city. Inactive since late 2021, its declining production values (Mwila et al., 2022) match well the TROPOMI-derived NO_2 emissions (R = 0.96, Fig. 2.f).

The six Copperbelt NO_2 emission point sources do not coincide with SO_2 enhancements, as shown by the map of mean TROPOMI SO_2 VCD values for the period between January 2019 and July 2022 (Fig. 3). The map shows SO_2 enhancements elsewhere: collocated with the Hwange coal power plant (Zimbawe), the Selous smelter (Zimbawe), and the Chingola and Mufulira smelters (Zambia).

Anthropogenic emissions from the inventory were compared to TROPOMI-derived emissions from our six point sources. Monthly inventory emissions from the following sectors were aggregated: power generation, industrial processes (including mining), road and non-road transportation, residential, fugitive fuel emissions, solvents application and production, and solid waste and wastewater handling. Emissions from the agriculture livestock, agriculture soils, and agriculture waste burning sectors would be part of the background over mines and cities and, thus, were excluded. Aggregated inventory emissions were converted to NO_2 ($NO_2 = NO_x / 1.32$; Beirle et al. (2019), Dix et al. (2022)). The highest inventory value among the nine data points coinciding spatially with each point source was selected; annual inventory means were calculated and compared to their background-removed TROPOMI-derived emissions counterparts (Table 1 and Fig. S5). The inventory underpredicts mine emissions by 61-96 %, generally overpredicts city emissions, and does not identify the annual trends in both TROPOMI-derived emissions and mine production.

5 Discussion

We have shown that NO_2 from copper/cobalt mining and other industrial activities can be identified and emissions quantified from satellite, even in the presence of high background values from biomass burning, soils, and lightening. Furthermore, we have demonstrated strong positive correlations between annual TROPOMI-derived NO_2 emissions and mine production/refinery throughput. These correlations are mine-dependent and cannot be extrapolated from mine to mine; differences in ore grades and equipment fuel efficiency are probably the main causes. As an example, lower-than-expected 2022 emissions from Lumwana, which reduced R from 1.00 (for 2019-2021) to 0.74 (for 2019-2022) (Fig. 2.c), can be traced to a new fleet of trucks and shovels commissioned in 2021 (Barrick, 2023) and in operation during 2022 (Lusaka Times, 2022).

As a reference, 2019 background-removed TROPOMI-derived NO_2 emissions from Ndola (0.044kg/s , after accounting for point source area) are equivalent to NO_2 emissions from the Miami Fort or the Intermountain coal power plants, both among the ten

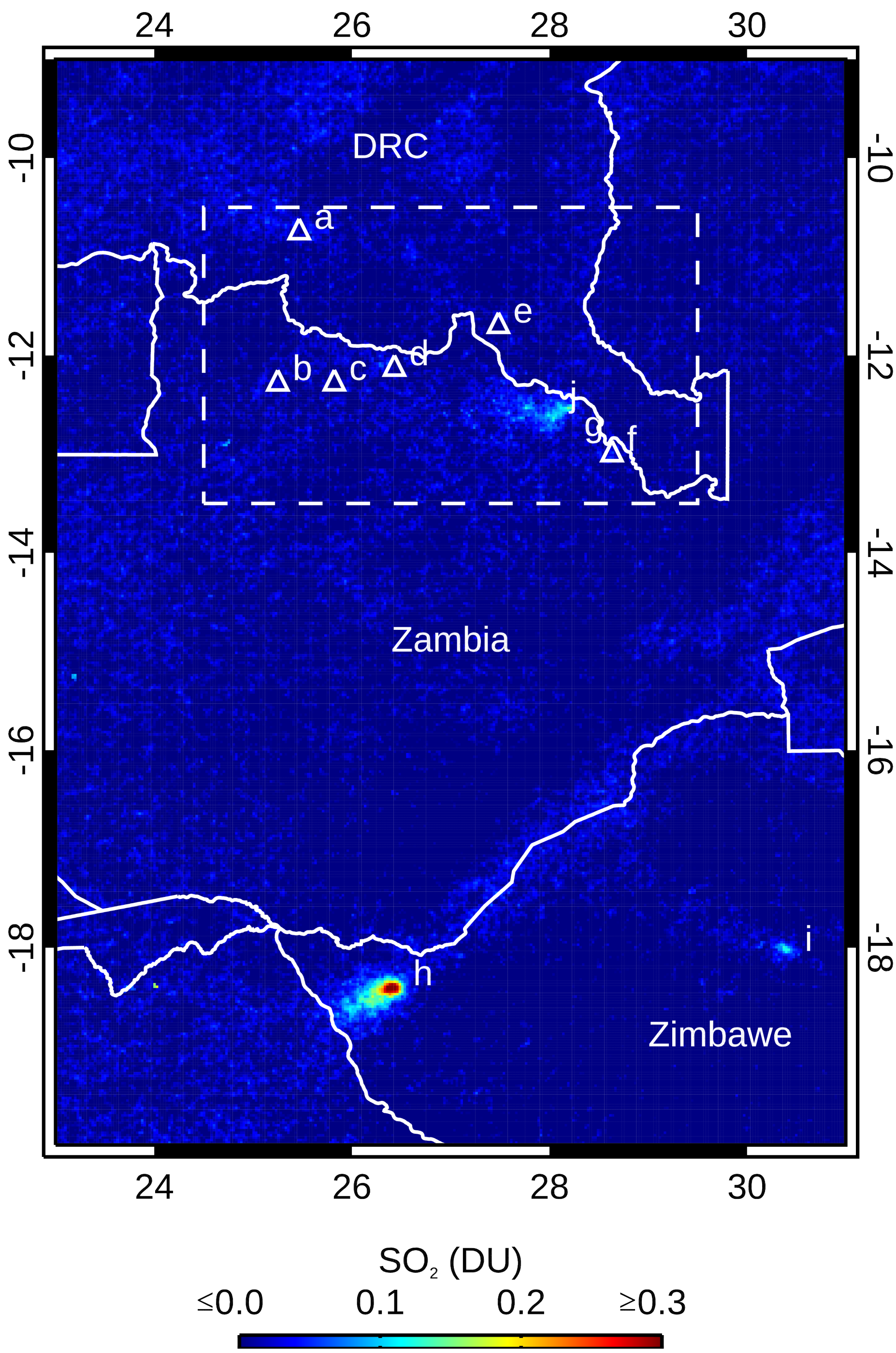

Figure 3. Mean TROPOMI-COBRA SO_2 VCD for January 2019 - July 2022. White triangles show the Copperbelt NO_2 emission point sources analyzed. (a) Kolwezi-Katanga. (b) Sentinel. (c) Lumwana. (d) Kansanshi. (e) Lubumbashi. (f) Ndola. (g) Kitwe. (h) Hwange coal power plant. (i) Selous smelter. (j) Chingola-Mufulira smelters. White lines show country boundaries. Dashed white lines show Copperbelt study area.

largest NO_x emitters in the USA that year (Beirle et al., 2021). Our results demonstrate that the impact of mining/oil refining on local air quality can be quantified using satellite data; this is particularly important for African regions where mining and other industrial activities proliferate without sufficient air quality monitoring.

We have analyzed the point sources with the highest mean annual TROPOMI-derived emissions in the Copperbelt; our maps do, however, show a string of NO_2 enhancements along the Ndola-Lubumbashi-Kolwezi corridor (Fig. 1) where relatively smaller copper/cobalt mining operations, both industrial and artisanal, exist. Future work should explore the detection limits of this method by analyzing some of these other NO_2 enhancements.

Ground emission measurements were unavailable; thus, we compared background-removed TROPOMI-derived NO_2 emissions to inventory data. Inventory values are lower (higher) for mines (cities) than their TROPOMI counterparts and do not capture the annual trends revealed by TROPOMI. The remoteness of the region, lack of field data, and relatively small size of the point sources may explain at least in part these discrepancies. NO_2 emissions derived from satellite measurements could improve the overall magnitude and temporal (seasonal, inter-annual) trends in inventory emissions. They could also be used to refine regional emission factors, which are not well defined for Africa.

We identified SO_2 enhancements coinciding with smelters and a coal power plant elsewhere, but none colocated with our NO_2 point sources (Fig. 3), despite the fact that some of them either include a smelter (Kansanshi, First Quantum (2023a)) or have one nearby (Lualaba, 40 km southeast of Kolwezi; Ivanhoe Mines (2021)). Lack of SO_2 enhancements indicates use of technologies to convert sulfur oxides released from the ore during smelting into sulfuric acid, a commercial byproduct (Hocking, 2005; Ialongo et al., 2018). The use of such technologies in the Kansanshi and Lualaba smelters has been documented by the mining companies involved (Gray et al., 2020; First Quantum, 2023b; Wang, 2020).

6 Conclusions

Understanding the environmental effects of high-impact minerals extraction and processing is of great relevance (Hund et al., 2020), particularly if the mining-related activities take place in close proximity to -or even inside of- population centers, as is the case in the Copperbelt region. We have shown for the first time that NO_2 emissions from copper and cobalt mining activities can be identified and measured using TROPOMI satellite data, even in the presence of high background NO_2; this is important in the absence of local air quality monitoring. Furthermore, we have shown, also for the first time, a strong positive correlation between TROPOMI-derived NO_2 emissions and mining/oil refining production data. We note that these correlations are mine-dependent and that changes in the mine's environment (ore grade, fuel efficiency) will affect such correlations, as observed in Lumwana. The lack of SO_2 enhancements colocated with our NO_2 point sources (enhancements identified, though, in power plants and smelters nearby) is consistent with SO_2 capture and transformation into sulfuric acid, which is then used in mining-related processes or commercialized.

Because the NO_2 emissions analyzed result from the combustion of fossil fuels by machinery (e.g., trucks, crushers, generators) used extensively in mining operations, these results are relevant to mining in general, regardless of the resource mined. They are also relevant to oil refineries, as shown in Ndola. We hypothesize that our findings apply to fossil-fuel intensive industries in general.

Our results show that NO_2 trend analysis can be used to predict mine production and refinery throughput before companies release their reports or in lieu of these reports in case of non-publicly traded companies, which are not required to publish their activity data. Insufficient emissions from mines claiming high production may be indicative of production from a different source. Thus, this method may be useful for improving traceability of minerals extracted in conflict areas and smuggled into the global supply chain despite existing traceability and tagging schemes, an issue highlighted in the most recent releases of the United Nations Yearbook (United Nations, 2019, 2022).

Open Research Section

Atmospheric data available as follows. TROPOMI NO_2 data (L2__NO2_) are publicly available via the ESA's S5P Pre-Ops interface (https://scihub.copernicus.eu/) using the credentials given there. TROPOMI SO2 COBRA data: https://distributions.aeronomie.be/?menu=68c9f961bc294141c215e3d64a6ae282#. ERA5 data: https://cds.climate.copernicus.eu/cdsapphttps://cds.climate.copernicus.eu/cdsapp#!/dataset/reanalysis-era5-single-levels-monthly-means?tab=form (hourly data on single levels) and https://cds.climate.copernicus.eu/cdsapp#!/dataset/reanalysis-era5-pressure-levels?tab=form (hourly data on pressure levels). CAMS-GLOB-ANT inventory data are publicly available via the https://eccad3.sedoo.fr/ interface following the instructions given there to create a free access account. Mining production data available from mining company reports as follows. First Quantum Minerals Ltd. (Sentinel, Kansanshi): https://s24.q4cdn.com/821689673/files/doc_downloads/2019-annual-report/First_Quantum_AR_2019.pdf (2019), https://s24.q4cdn.com/821689673/files/doc_downloads/2020-annual-report/First_Quantum_2020_Annual_Report.pdf (2020), https://www.firstquantum-2021-annual-report.com/_files/ugd/acdda3_c51ed134aa184e259d61a629344f98e7.pdf (2021), https://www.first-quantum.com/files/doc_downloads/2022-annual-report/First-Quantum-2022- AR-online.pdf (2022). Barrick Gold Corporation (Lumwana): https://s25.q4cdn.com/322814910/files/doc_financial/annual_reports/2019/Barrick-Annual- Report-2019.pdf (2019), https://s25.q4cdn.com/322814910/files/doc_financial/annual_reports/2020/Barrick-Annual- Report-2020.pdf (2020), https://s25.q4cdn.com/322814910/files/doc_financial/annual_reports/2021/Barrick_Annual_Report_2021.pdf (2021), https://s25.q4cdn.com/322814910/files/doc_financial/annual_reports/2022/Barrick_Annual_Report_2022.pdf (2022). Zijing Mining (Kolwezi): https://www.zijinmining.com/upload/file/2020/09/14/9c97a89f8e9c4c59a13f2404f3bb1096.pdf (2019), https://www.zijinmining.com/upload/file/2021/06/09/538a46cc4831452e97b30cae55c9cf97.pdf (2020), https://www.zijinmining.com/upload/file/2022/06/20/771c971d76154257882f58ed03643c07.pdf (2021; no 2022 annual report available at the time of writing). Glencore (Katanga): https://www.glencore.com/.rest/api/v1/documents/5a08fe1942f92df7f2301ac3681e23aa/glen- 2019-annual-report-interactive.pdf?download=true (2019), https://www.glencore.com/.rest/api/v1/documents/3505497f3cb94b24f0c79f5ba32b293b/Glencore_AR20_Interactive+%281%29.pdf?download=true (2020), https://www.glencore.com/.rest/api/v1/documents/ce4fec31fc81d6049d076b15db35d45d/GLEN-

2021-annual-report-.pdf?download=true (2021), https://www.glencore.com/.rest/api/v1/documents/ded10fa92974aa388a43aa9f86f483e9/GLEN-2022-Annual-Report.pdf (2022).

ERA5 data are produced by C3S and CAMS. Contains modified information from C3S and CAMS [2019-2021]. Neither the European Commission nor ECMWF is responsible for any use that may be made of the Copernicus information data contained in this study.

Acknowledgments

SMA thanks William Atkinson for sharing his deep knowledge of minerals and mining; Carol Atkinson for her insights and inspiring curiosity; Louisa Emmons for advice regarding models; David Edwards and Bill Randel for helpful NCAR in-house comments.

This material is based upon work supported by the National Center for Atmospheric Research, which is a major facility sponsored by the National Science Foundation under Cooperative Agreement No. 1852977.

References

Africa Intelligence. (2021). *Lubumbashi slag heap locals fume over pollution.* Retrieved from https://www.africaintelligence.com/central-africa/2021/05/25/lubumbashi-slag-heap-locals-fume-over-pollution,109668540-art (last access: 19 February 2023)

Allen, M. (2021). *Mining Energy Consumption 2021* (Tech. Rep.). ENGECO Pte. Ltd. Retrieved from https://www.ceecthefuture.org/resources/mining-energy-consumption-2021 (last access: 21 February 2023)

Atibu, E. K., Devarajan, N., Laffite, A., Giuliani, G., Salumu, J. A., Muteb, R. C., ... Pore, J. (2016). Assessment of trace metal and rare earth elements contamination in rivers around abandoned and active mine areas. The case of Lubumbashi River and Tshamilemba Canal, Katanga, Democratic Republic of the Congo. *CHEMIE DER ERDE-GEOCHEMISTRY*, *76*(3), 353-362. doi: 10.1016/j.chemer.2016.08.004

Barrick. (2023). *Annual reports.* Retrieved from https://www.barrick.com/English/investors/default.aspx (last access: 08 February 2023)

Beirle, S., Boersma, K. F., Platt, U., Lawrence, M. G., & Wagner, T. (2011). Megacity emissions and lifetimes of nitrogen oxides probed from space. *SCIENCE*, *333*(6050), 1737-1739. doi: 10.1126/science.1207824

Beirle, S., Borger, C., Doerner, S., Eskes, H., Kumar, V., de Laat, A., & Wagner, T.

(2021). Catalog of NO_x emissions from point sources as derived from the divergence of the NO_2 flux for TROPOMI. *EARTH SYSTEM SCIENCE DATA*, *13*(6), 2995-3012. doi: 10.5194/essd-13-2995-2021

Beirle, S., Borger, C., Drner, S., Li, A., Hu, Z., Liu, F., . . . Wagner, T. (2019). Pinpointing nitrogen oxide emissions from space. *Science Advances*, *5*, eaax9800. doi: 10.1126/sciadv.aax9800

BIRA-IASB. (2021). *Global map of nitrogen dioxide (NO_2).* Retrieved from https://uv-vis.aeronomie.be/data/tropomi_posters/posterTROPOMI_NO2_2018_2020.pdf (last access: 7 April 2023)

Carn, S. A., Krueger, A. J., Krotkov, N. A., Yang, K., & Levelt, P. F. (2007). Sulfur dioxide emissions from Peruvian copper smelters detected by the Ozone Monitoring Instrument. *GEOPHYSICAL RESEARCH LETTERS*, *34*(9). doi: 10.1029/2006GL029020

de Foy, B., & Schauer, J. J. (2022). An improved understanding of NO_x emissions in South Asian megacities using TROPOMI NO_2 retrievals. *ENVIRONMENTAL RESEARCH LETTERS*, *17*(2). doi: 10.1088/1748-9326/ac48b4

Dix, B., Francoeur, C., Li, M., Serrano-Calvo, R., Levelt, P. F., Veefkind, J. P., . . . de Gouw, J. (2022). Quantifying NO_x Emissions from US Oil and Gas Production Regions Using TROPOMI NO_2. *ACS EARTH AND SPACE CHEMISTRY*, *6*(2), 403-414. doi: 10.1021/acsearthspacechem.1c00387

Eskes, H., van Geffen, J., Boersma, F., Eichmann, K.-U., Apituley, A., Pedergnana, M., . . . Loyola, D. (2022). *Sentinel-5 precursor/TROPOMI Level 2 Product User Manual Nitrogen dioxide* (Tech. Rep. Nos. 2.4.0, 2021-07-11). Netherlands Institute for Space Research (SRON).

Eskes, H. J., & Eichmann, K.-U. (2021). *S5P mission performance centre nitrogen dioxide (L2 NO_2) readme* (Tech. Rep. Nos. 2.1, 2021-11-17). Netherlands Institute for Space Research (SRON).

Fioletov, V., McLinden, C. A., Griffin, D., Abboud, I., Krotkov, N., Leonard, P. J. T., . . . Carn, S. (2023). Version 2 of the global catalogue of large anthropogenic and volcanic SO_2 sources and emissions derived from satellite measurements. *EARTH SYSTEM SCIENCE DATA*, *15*(1), 75-93. doi: 10.5194/essd-15-75-2023

Fioletov, V., Mclinden, C. A., Griffin, D., Theys, N., Loyola, D. G., Hedelt, P., . . . Li, C. (2020). Anthropogenic and volcanic point source SO_2 emissions derived from TROPOMI on board Sentinel-5 Precursor: first results. *ATMOSPHERIC CHEMISTRY AND PHYSICS*, *20*(9), 5591-5607. doi: 10.5194/acp-20-5591-2020

Fioletov, V. E., McLinden, C. A., Krotkov, N., Yang, K., Loyola, D. G., Valks, P., . . . Martin, R. V. (2013). Application of OMI, SCIAMACHY, and GOME-2 satellite SO_2 retrievals for detection of large emission sources. *JOURNAL OF GEOPHYSICAL RESEARCH-ATMOSPHERES*, *118*(19), 11399-11418. doi: 10.1002/jgrd.50826

First Quantum. (2023a). *Annual reports.* Retrieved from https://www.first-quantum.com/English/investors/financial-information/default.aspx (last access: 08 February 2023)

First Quantum. (2023b). *Kansanshi: smelter.* Retrieved from https://www.first-quantum.com/English/our-operations/default.aspx#module-operation--kansanshi (last access: 24 March 2023)

Glencore. (2023). *Annual reports.* Retrieved from https://www.glencore.com/publications (last access: 08 February 2023)

Goldberg, D. L., Lu, Z., Streets, D. G., de Foy, B., Griffin, D., McLinden, C. A., . . . Eskes, H. (2019). Enhanced Capabilities of TROPOMI NO_2: Estimating NO_x from North American Cities and Power Plants. *ENVIRONMENTAL SCIENCE & TECHNOLOGY*, *53*(21), 12594-12601. doi: 10.1021/acs.est.9b04488

Granier, C., S. Darras, H. Denier van der Gon, J. Doubalova, N. Elguindi, B. Galle, M. Gauss, M. Guevara, J.-P. Jalkanen, J. Kuenen, C. Liousse, B. Quack, D. Simpson, K. Sindelarova, The Copernicus Atmosphere Monitoring Service global and regional emissions, Copernicus Atmosphere Monitoring Service (CAMS) report, doi:10.24380/d0bn-kx16, 2019

Gray, D., Lawlor, M., & Briggs, A. (2020). *Kansanshi Operations, North West Province, Zambia, NI 43-101 Technical Report, June 2020* (Tech. Rep.). First Quantum Minerals Ltd.

Gulley, A. L. (2022). One hundred years of cobalt production in the Democratic Republic of the Congo. *Resources Policy*, *79*. doi: 10.1016/j.resourpol.2022.103007

Hersbach, H., Bell, B., Berrisford, P., Hirahara, S., Horanyi, A., Munoz-Sabater, J., ... Thepaut, J.-N. (2020). The ERA5 global reanalysis. *QUARTERLY JOURNAL OF THE ROYAL METEOROLOGICAL SOCIETY*, *146*(730), 1999-2049. doi: 10.1002/qj.3803

Hocking, M. B. (2005). Ore Enrichment and Smelting of Copper. In M. B. Hocking (Ed.), *Handbook of Chemical Technology and Pollution Control* (Third ed., p. 391-420). San Diego: Academic Press. doi: 10.1016/B978-012088796-5/50016-8

Hund, K., LaPorta, D., Fabregas, T., Laing, T., & Drexhage, J. (2020). *Minerals for climate action: The mineral intensity of the clean energy transition.* The World Bank. Retrieved from https://pubdocs.worldbank.org/en/961711588875536384/Minerals-for-Climate-Action-The-Mineral-Intensity-of-the-Clean-Energy-Transition.pdf

Ialongo, I., Fioletov, V., McLinden, C., Jafs, M., Krotkov, N., Li, C., & Tamminen, J. (2018). Application of satellite-based sulfur dioxide observations to support the cleantech sector: Detecting emission reduction from copper smelters. *Environmental Technology & Innovation*, *12*, 172-179. doi: 10.1016/j.eti.2018.08.006

Ivanhoe Mines. (2021). *Agreement signed with nearby Lualaba Copper Smelter to produce 99% blister copper in the Democratic Republic of Congo.* Retrieved from http://www.sulphuric-acid.com/sulphuric-acid-on-the-web/acid\%20plants/Lualaba-Copper-Smelter.htm (last access: 22 February 2023)

Kayembe-Kitenge, T., Lubala, T. K., Obadia, P. M., Chimusa, P. K., Nawej, C. K., Nkulu, C. B. L., ... Nemery, B. (2019). Holoprosencephaly: A case series from an area with high mining-related pollution. *BIRTH DEFECTS RESEARCH*, *111*(19), 1561-1563. doi: 10.1002/bdr2.1583

Krueger, A. (1983). SIGHTING OF EL-CHICHON SULFUR-DIOXIDE CLOUDS WITH THE NIMBUS-7 TOTAL OZONE MAPPING SPECTROMETER. *SCIENCE*, *220*(4604), 1377-1379. doi: 10.1126/science.220.4604.1377

Labzovskii, L. D., Belikov, D. A., & Damiani, A. (2022). Spaceborne NO_2 observations are sensitive to coal mining and processing in the largest coal basin of Russia. *SCIENTIFIC REPORTS*, *12*(1). doi: 10.1038/s41598-022-16850-8

Leue, C., Wenig, M., Wagner, T., Klimm, O., Platt, U., & Jahne, B. (2001). Quantitative analysis of NO_x emissions from Global Ozone Monitoring Experiment satellite image sequences. *JOURNAL OF GEOPHYSICAL RESEARCH-ATMOSPHERES*, *106*(D6), 5493-5505. (2nd AGU Chapman Conference on Water Vapor in the Climate System, POTOMAC, MD, OCT 12-15, 1999) doi: 10.1029/2000JD900572

Lusaka Times. (2022). *Barrick hoping to extend Lumwana mine to 2042.* Retrieved from https://www.lusakatimes.com/2022/10/31/barrick-hoping-to-extend-lumwana-mine-to-2042/ (last access: 28 February 2023)

Mwila, A. M., et al. (Eds.). (2022). *2021 Energy Sector Report* (Tech. Rep.). Energy Regulation Board, Zambia.

Mwitwa, J., German, L., Muimba-Kankolongo, A., & Puntodewo, A. (2012). Governance and sustainability challenges in landscapes shaped by mining:

Mining-forestry linkages and impacts in the Copper Belt of Zambia and the DR Congo. *FOREST POLICY AND ECONOMICS*, *25*, 19-30. doi: 10.1016/j.forpol.2012.08.001

Myhre, G., Shindell, D., Bron, F.-M., Collins, W., Fuglestvedt, J., Huang, J., . . . Zhang, H. (2013). Anthropogenic and natural radiative forcing. In T. F. Stocker et al. (Eds.), *Climate Change 2013: The Physical Science Basis. Contribution of Working Group I to the Fifth Assessment Report of the Intergovernmental Panel on Climate Change* (pp. 659–740). Cambridge, UK: Cambridge University Press. doi: 10.1017/CBO9781107415324.018

Peˇsa, I. (2022). Mining, Waste and Environmental Thought on the Central African Copperbelt, 1950-2000. *ENVIRONMENT AND HISTORY*, *28*(2), 259-284. doi: 10.3197/096734019X15755402985703

Pommier, M. (2022). Estimations of NO_x emissions, NO_2 lifetime and their temporal variation over three British urbanised regions in 2019 using TROPOMI NO_2 observations. *ENVIRONMENTAL SCIENCE-ATMOSPHERES*. doi: 10.1039/d2ea00086e

Population Stat. (2023). *World statistical data.* Retrieved from https://populationstat.com/ (last access: 18 February 2023)

Richter, A., Begoin, M., Hilboll, A., & Burrows, J. P. (2011). An improved NO_2 retrieval for the GOME-2 satellite instrument. *Atmospheric Measurement Techniques*, *4*(6), 1147–1159. Retrieved from https://amt.copernicus.org/articles/4/1147/2011/ doi: 10.5194/amt-4-1147-2011

Richter, A., Burrows, J., Nuss, H., Granier, C., & Niemeier, U. (2005). Increase in tropospheric nitrogen dioxide over China observed from space. *NATURE*, *437*(7055), 129-132. doi: 10.1038/nature04092

Shedd, K. B. (2022). *Cobalt. In: 2022 Mineral Commodity Summaries.* (Tech. Rep.). U.S. Geological Survey.

STL. (2023). *Statistiques de production.* Retrieved from http://www.stlgcm.com/ (last access: 19 February 2023)

The Carter Center. (2023). *Mining royalty statistics for the province of H-Katanga / Cumulative 2021.* Retrieved from https://congomines.org/reports/ (last access: 18 February 2023)

Theys, N. (2022). *S5P COBRA Sulphur Dioxide (L2 SO2CBR) Readme* (Tech. Rep. Nos. 1.0.0, 2022-09-14). Royal Belgian Institute for Space Aeronomy (BIRA-IASB).

Theys, N., Fioletov, V., Li, C., De Smedt, I., Lerot, C., McLinden, C., . . . Van Roozendael, M. (2021). A sulfur dioxide Covariance-Based Retrieval Algorithm (COBRA): application to TROPOMI reveals new emission sources. *ATMOSPHERIC CHEMISTRY AND PHYSICS*, *21*(22), 16727-16744. doi: 10.5194/acp-21-16727-2021

United Nations. (2019). (O. F. Summerell et al., Eds.). New York, NY, USA: United Nations Department of Global Communications. Retrieved from https://www.unmultimedia.org/searchers/yearbook/page_un2.jsp?volume=2014&page=1

United Nations. (2022). New York, NY, USA: United Nations Department of Global Communications. Retrieved from https://www.un.org/en/yearbook/prepress

U.S. Bureau of Mines (Ed.). (1993). *1990 Minerals Yearbook: Mineral Industries of Africa* (Tech. Rep.). U.S. Bureau of Mines.

Van Brusselen, D., Kayembe-Kitenge, T., Mbuyi-Musanzayi, S., Kasole, T. L., Ngombe, L. K., Obadia, P. M., . . . Nemery, B. (2020). Metal mining and birth defects: a case-control study in Lubumbashi, Democratic Republic of the Congo. *LANCET PLANETARY HEALTH*, *4*(4), E158-E167.

van Geffen, J., Boersma, K. F., Eskesl, H., Sneep, M., ter Linden, M., Zara, M., & Veefkind, J. P. (2020). S5P TROPOMI NO_2 slant column retrieval: method, stability, uncertainties and comparisons with OMI. *ATMOSPHERIC MEASUREMENT TECHNIQUES*, *13*(3), 1315-1335. doi: 10.5194/amt-13-1315-2020

Veefkind, J. P., Aben, I., McMullan, K., Forster, H., de Vries, J., Otter, G., . . . Levelt, P. F. (2012). TROPOMI on the ESA Sentinel-5 Precursor: A GMES mission for global observations of the atmospheric composition for climate, air quality and ozone layer applications [Article]. *Remote Sensing of Environment*, *120*(SI), 70-83. doi: {10.1016/j.rse.2011.09.027}

Wang, R. (2020). *CNMC-invested and constructed mining, copper smelting projects go into production.* Retrieved from http://en.sasac.gov.cn/2020/01/22/c_12660.htm (last access: 24 March 2023)

World Health Organization. (2021). *WHO global air quality guidelines: particulate matter (PM2.5 and PM10), ozone, nitrogen dioxide, sulfur dioxide and carbon monoxide* [Publications]. World Health Organization.

Zhang, Y., Li, C., Krotkov, N. A., Joiner, J., Fioletov, V., & McLinden, C. (2017). Continuation of long-term global SO_2 pollution monitoring from OMI to OMPS. *ATMOSPHERIC MEASUREMENT TECHNIQUES*, *10*(4). doi: 10.5194/amt-10-1495-2017

Zijin. (2023). *Annual reports.* Retrieved from https://www.zijinmining.com/investors/Annual-Reports.jsp (last access: 08 February 2023)

TROPOMI-derived NO_2 emissions from copper/cobalt mining and other industrial activities in the Copperbelt (DRC and Zambia)

S. Martínez-Alonso[1], J. P. Veefkind[2,3], B. Dix[4], B. Gaubert[1], N. Theys[5], C. Granier[4,6,7], A. Soulié[6], S. Darras[8], H. Eskes[2], W. Tang[1], H. Worden[1], J. de Gouw[4,9], and P. F. Levelt[1,2,3]

[1]ACOM-NCAR, Boulder, Colorado, USA
[2]KNMI, De Bilt, The Netherlands
[3]Department of Civil Engineering and Geosciences, Technical University of Delft, Delft, The Netherlands
[4]CIRES, University of Colorado, Boulder, Colorado, USA
[5]BIRA-IASB, Brussels, Belgium
[6]Laboratoire dA´erologie, CNRS, University of Toulouse UPS, Toulouse, France
[7]NOAA-CSL, Boulder, Colorado, USA
[8]Observatoire Midi-Pyr´en´ees, Toulouse, France
[9]Department of Chemistry, University of Colorado Boulder, Boulder, Colorado, USA

Key Points:

- We quantified annual 2019-2022 TROPOMI-derived NO_2 emissions from six point sources in the Copperbelt, despite high background emissions.
- Annual TROPOMI-derived NO_2 emissions from these point sources are strongly correlated with annual mine/oil refinery production.
- Lack of elevated SO_2 at these point sources is consistent with SO_2 capture and production of sulfuric acid, a profitable byproduct.

Corresponding author: Sara Martínez-Alonso, sma@ucar.edu

Abstract

We have analyzed TROPOMI data over the Copperbelt mining region (Democratic Republic of Congo and Zambia). Despite high background values, we find that annual 2019-2022 means of TROPOMI NO_2 show local enhancements consistent with six point sources (mines and cities) where high-emission industrial activities take place. We have quantified annual NO_2 emissions for the six sources, identified temporal trends in these emissions, and found strong correlations with mine/refinery production data. CAMS-GLOBANT v5 inventory emissions are lower than TROPOMI-derived emissions by 61-96 % and lack the temporal trends observed in TROPOMI and mine/oil refinery production. Lack of TROPOMI SO_2 enhancements over the point sources analyzed indicates SO_2 capture and transformation into sulfuric acid, a profitable byproduct. These results demonstrate the potential for satellite monitoring of mining/oil refining activity which impacts the air quality of local communities. This is particularly important for Africa, where mining is increasing aggressively.

Plain Language Summary

We show that air pollution from copper/cobalt mines and oil refineries can be identified and measured from satellite, even in the presence of high background pollution from biomass burning and other sources; our findings may apply as well to other industries that consume large quantities of fossil fuels. This is important for monitoring the air quality of local communities, particularly when these industrial activities take place in close proximity to population centers, as is the case in the Copperbelt and, in general, in other African regions where mining and related industrial activities proliferate without sufficient air quality monitoring. Additionally, we show for the first time that the amount of air pollution measured by TROPOMI is strongly correlated with mine/refinery production. Studies like this can be used to estimate mine/refinery production before companies release their annual reports or (as is the case with non-publicly traded companies) in the absence of such reports. Insufficient emissions from mines claiming high production may be indicative of production from a different source. Thus, this method may help improve the traceability of minerals extracted in conflict areas and smuggled into the global supply chain despite existing traceability and tagging schemes.

1 Introduction

The Copperbelt, a mining region straddling the DRC (Democratic Republic of Congo) and Zambia, is currently of great strategic interest because it is the world's largest cobalt producer and holds almost half of the world reserves (Shedd, 2022). Cobalt production in the Copperbelt (mostly in the DRC) has increased $\sim$600% between 1990 and 2021 (U.S. Bureau of Mines, 1993; Shedd, 2022), driven by its use in lithium-ion batteries which power mobile phones, laptops, and electric cars. Access to the Copperbelt's cobalt is becoming a matter of national and global energy security (Gulley, 2022). Cobalt is, however, a byproduct of copper mining; copper is the main ore (by volume) extracted in the Copperbelt. Previous studies have documented the impact of cobalt and/or copper mining in the region's soils and water (Atibu et al., 2016), land use (Mwitwa et al., 2012), and neonatal health (Kayembe-Kitenge et al., 2019; Van Brusselen et al., 2020). The impact on local air quality remained unknown. Here we quantify the effect of increasing mining activity on the air quality of this region using TROPOMI (TROPOspheric Monitoring Instrument) satellite measurements (Veefkind et al., 2012) of NO_2 (nitrogen dioxide); TROPOMI SO_2 (sulfur dioxide) is also analyzed. Both gases are atmospheric pollutants (World Health Organization, 2021) relevant to air quality monitoring and forecasting. They are also considered short-lived climate forcers, important for understanding climate (Myhre et al., 2013).

NO_x (NO_2 + NO, two species closely intertwined by oxidation and reduction reactions), has both anthropogenic (fossil fuel combustion, biomass burning) and natural (microbial activity in soils, lightning, wildfires) sources. Mining-related NO_x is produced by high-temperature combustion of fuel used by trucks and other heavy machinery as well as by electric generators. The main sink of NO_x is the hydroxyl radical (OH), with which it reacts within hours in the presence of light. NO_x has a negative impact on air quality, both directly and as a precursor to tropospheric ozone and particulate matter. It is damaging to human health (affecting mostly the respiratory system) and crops, and contributes to the formation of smog and acid rain. Hereafter we discuss NO_2, the NO_x component measurable from satellite.

Measuring global and regional NO_2 was made possible by satellite instruments such as GOME (Global Ozone Monitoring Experiment), SCIAMACHY (SCanning Imaging Absorption SpectroMeter for Atmospheric CHartographY), OMI (Ozone Monitoring Instrument), and GOME-2, (Leue et al., 2001; Richter et al., 2005; Beirle et al., 2011; Richter et al., 2011). Labzovskii et al. (2022) reported regional-scale correlation between OMI NO_2 column values from heavy industry, including mining, and a coal production inter-annual variability index for the Siberian Kuzbass Basin. Thanks to its higher spatial resolution, TROPOMI allows for the measurement of NO_2 over smaller domains such as gas and oil fields (Dix et al., 2022), cities (Goldberg et al., 2019; Pommier, 2022; de Foy & Schauer, 2022), and power plants (Beirle et al., 2019, 2021; Goldberg et al., 2019; Dix et al., 2022; de Foy & Schauer, 2022).

SO_2 results from both anthropogenic (e.g., coal combustion, smelting of sulfur-rich ores) and natural (volcanism, marine biological processes) sources. It contributes to acid rain and particle formation. Exposure to SO_2 is harmful to human health, damages foliage, and impedes plant growth. Previous studies showed that SO_2 emissions could be estimated using satellite data from TOMS (Total Ozone Mapping Spectrometer), GOME, OMI, SCIAMACHY, and OMPS (Ozone Mapping and Profiler Suite) (Krueger, 1983; Carn et al., 2007; V. E. Fioletov et al., 2013; Zhang et al., 2017). V. Fioletov et al. (2020, 2023) reported TROPOMI-based emission estimates of SO_2 from power plants, volcanoes, oil and gas fields, and smelters.

We show that copper/cobalt mining-related activities, among others, can be identified and their NO_2 emissions quantified based on TROPOMI data even in the presence of high background values from biomass burning and other sources (BIRA-IASB, 2021). Additionally, we identify inter-annual trends in TROPOMI-derived NO_2 emissions that are strongly correlated with mining and oil refinery production. Next we describe the datasets (Sect. 2) and methodology (Sect. 3) used in this study, we present our results (Sect. 4), and discuss their relevance (Sect. 5). Conclusions are offered in Sect. 6.

2 Datasets

TROPOMI, onboard the European Space Agency's Sentinel-5 Precursor satellite (Veefkind et al., 2012), provides quasi-global daily coverage at high spatial resolution (3.5 x 5.5 km^2 for our species of interest). This is a nadir-viewing imaging spectrometer in a sun-synchronous orbit at 824 km of altitude, with 13:30 LST Equator-crossing time, and 2600 km swath width. TROPOMI measures radiances in the ultraviolet, visible, and reflected infrared, from which concentrations of trace gases as well as cloud and aerosol properties are derived. Here we focus on TROPOMI measurements of tropospheric NO_2 and SO_2, two pollutants produced by mining-related activities. NO_2 is retrieved from TROPOMI radiance measurements in the visible portion of the spectrum (400-496 nm) (van Geffen et al., 2020; H. J. Eskes & Eichmann, 2021; H. Eskes et al., 2022). We used daily TROPOMI NO_2 tropospheric column data from version 2 for the period between 1 January 2019 and 31 December 2022. We also analyzed TROPOMI SO_2 data retrieved with the Covariance-Based Retrieval Algorithm (COBRA, Theys et al. (2021)) from ultraviolet-visible radiances (310.5-326 nm) (Theys, 2022) for the 1 January 2019 - 31 July 2022 period; more recent data were unavailable at the time of writing.

Meteorological information needed to derive emissions from TROPOMI NO_2 VCD (vertical column density) was obtained from reanalysis data. By combining measurements and model results, reanalyses datasets provide consistent and gapless global coverage of essential climate variables. We used hourly ERA5 (ECMWF Reanalysis v5) data (Hersbach et al., 2020) provided at 0.25° x 0.25° resolution and generated by the Copernicus Climate Change Service at the European Center for Medium-Range Weather Forecasts.

Due to the unavailability of ground measurements, we compared inventory data to TROPOMI-derived NO2 emissions. Emission inventories are compilations of amounts of air pollutants released into the atmosphere, segregated by source and time period. We used 2019-2021 data from the CAMS-GLOB-ANT (Copernicus Atmosphere Monitoring Service Global Anthropogenic) emissions inventory version 5, an extension of version 4.2 (Granier et al., 2019). Inventory emissions for 2022 were unavailable at the time of writing. We focused on monthly NOx emissions, provided at 0.1° x 0.1° resolution.

Mine production data were obtained from the annual reports of publicly traded mining companies; these reports are mandated by official regulatory bodies such as the Securities and Exchange Commission in the United States and the Securities and Futures Commission in Hong Kong. Private mining companies are not required to disclose their production data. The specifics of the information available in these reports varies greatly.

3 Methodology

To identify potential emission point sources such as mines, we produced annual means from daily TROPOMI NO_2 VCD for the Copperbelt study area (-10.5°N to -13.5°N, 24.5°E to 29.5°E). Temporal averaging enhances the signal from constantly emitting sources while dampening more sporadic, background emissions from biomass burning, soils, and lightning.

Once the point sources were identified, we calculated daily TROPOMI-derived NO_2 emissions for the study area using the divergence method (Beirle et al., 2019; Dix et al., 2022) with some modifications described below. This method derives emission based on a divergence term and a sink term, which account for wind dispersion effects and NO_2 depletion by OH, respectively. A detailed description of the derivation can be found in Dix et al. (2022). To calculate daily emissions we regridded daily VCD values to a common 0.025° x 0.025° grid. We filtered TROPOMI measurements to avoid clouds, errors, and problematic retrievals by using only those with quality assurance value ≥ 0.75 (H. Eskes et al., 2022); retrievals with solar zenith angle $> 60°$ were rejected. Hourly values of fields (longitudinal and latitudinal horizontal wind at 100 m from the ground, pressure, and temperature) required for the emissions calculation were obtained from ERA5 reanalysis. All ERA5 fields were resampled to 0.025° x 0.025° spatial resolution and interpolated to the passing time of the closest (spatially and temporally) TROPOMI observation. Fields provided on pressure levels were interpolated to an altitude of 100 m above the ground. In our implementation, OH lifetime was calculated for each data point based on the solar zenith angle of the closest TROPOMI retrieval. Daily emissions were averaged into annual means.

To calculate the actual NO_2 emissions released from each point source, background NO_2 emissions must be quantified and removed from the raw (non-background corrected) emissions. Several background removal approaches are possible: Beirle et al. (2019) subtracted from the emissions their 10th percentile value, Dix et al. (2022) removed the mode of a Gaussian curve fit to them. We find that the former is better suited to study regions with homogeneous background emissions and that results from the latter are highly dependent on how the Gaussian curve is defined. Similarly, statistics derived from two-dimensional

Gaussians fitted to the point source emissions (Beirle et al., 2019) were, in our case, highly dependent on location and size of the area selected to perform the fit. Our approach consisted of calculating annual statistics (mean and standard deviation) for each point source plume as well as for its local background area: a ~1° x 1° region surrounding each point source, excluding the point source plume. The location and extent of the point source plumes were identified based on an empirical threshold (0.37 kg km^{-2} h^{-1}) applied to mean raw emissions from the 2019-2022 period. Annual means of background-removed emissions were calculated for each point source by subtracting its mean background value from its mean raw emission value.

Dix et al. (2022) described in detail the effects of individual parameters (e.g., background correction, wind level, wind data source, OH lifetime, VCD thickness) on the results obtained using this method. We investigated ERA5 wind data uncertainty effects by using the spread of its wind field 10 member ensemble to perturb 2020 NO_2 emissions. The spread provides an estimate of relative, random uncertainty; ensemble, mean, and spread are part of the ERA5 dataset. The results show that ERA5 wind uncertainty produces small changes in raw NO_2 emission (< 4 %; Table S1 and Fig. S1).

4 Results

Six distinct point sources are clearly visible in the mean 2019-2022 TROPOMI NO_2 VCD map (Fig. 1; Fig. S2 shows annual mean VCD maps). Four of the point sources correspond to large copper (Sentinel, a.k.a. Trident; Lubumbashi; Kansanshi) or copper-cobalt (Kolwezi and adjacent Katanga) open-pit mines. The remaining two point sources coincide with cities (Lubumbashi and Ndola) where we infer that high-emission industrial activities take place, as explained below. Latitudinal profiles of mean annual VCD across each point source (Fig. 1) show that background NO_2 remains nearly constant year to year while the point sources (well defined, narrow peaks of fixed location) vary in magnitude. TROPOMI emission results (Table 1 and Fig. S3) reinforce these observations. TROPOMI NO_2 mostly increased with time at all the point sources but one, Ndola, where background-removed emissions decreased by > 70 % between 2019 and 2022.

To understand these inter-annual trends in NO_2 emissions, we compared background-removed TROPOMI-derived emissions to mine production data where available (Table 1 and Fig. 2). Most of the energy consumed in copper or copper-cobalt mining, including electricity, is generated by diesel fuel combustion. Mining equipment consumes ~60 % of the total energy; comminution ~36 %; flotation, filtering, and drying ~4 % (Allen, 2021). Limited data relevant to energy consumption is provided in mining company reports; we found the best proxy for energy (i.e., diesel) consumed to be amount of ore and waste mined. Panels b, c, and d in Fig. 2 show strong positive correlation between annual values of total ore plus waste mined versus NO_2 emissions for the Sentinel, Lumwana, and Kansanshi mines ($R = 0.84$, 0.74, and 0.79, respectively). Amount of copper produced (highly dependent on ore grade, among other factors, and thus, a less-desirable proxy) was used for the Kolwezi-Katanga mines (Fig. 2.a) for lack of ore and waste data ($R = 0.84$).

The remaining two point sources coincide with some of the largest cities in the study area: Lubumbashi (DRC, population > 2.6 x 10^6) and Ndola (Zambia, population > 0.5 x 10^6). To discard the hypothesis that their emissions are due to urban activity alone, we quantified NO_2 emissions for two additional cities of similar size: Mbuji-Mayi (DRC, population > 2.7 x 10^6), located 750 km northwest of Lubumbashi; and Kitwe (Zambia, population > 0.7 x 10^6), 50 km northwest of Ndola (labeled g in Fig. 1 map). (Population data are for 2022 urban areas (Population Stat, 2023).) The results (Fig. 1, Table S2, and Fig. S4) show that neither the magnitude of VCD or emissions, the spatial extent of the plumes, or the temporal emission trends from Lubumbashi and Ndola can be explained by urban activity alone. Background-removed NO_2 emissions from Lubum-

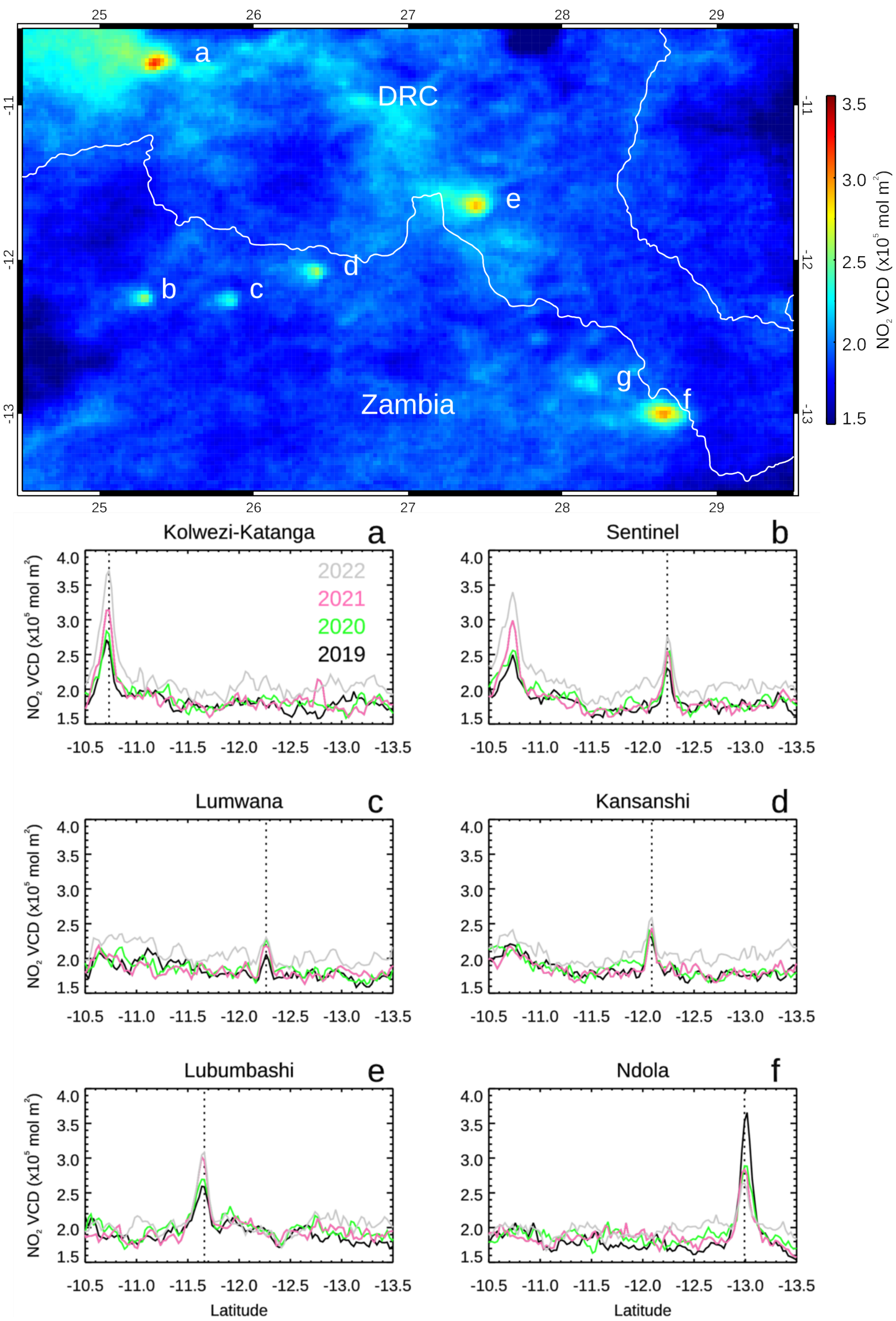

Figure 1. (Top) 2019-2022 mean of TROPOMI NO_2 VCD for the Copperbelt study region. Labels a through f show the six point sources analyzed. Label g shows the location of Kitwe City. White lines indicate country borders. (Bottom) Annual means of TROPOMI NO_2 VCD along latitudinal profiles centered at each of the six point sources, shown by vertical dotted lines. Labels as above. Profiles are color-coded according to year.

Table 1. Production and NO_2 emissions (TROPOMI background-removed, TROPOMI background, inventory) for six Copperbelt point sources. Ore, waste, and copper produced are in ktonnes; copper grade in percentage. Kansanshi reports provide separate copper grade values for sulfide, mixed, and oxide ores. Throughput (slag processed in Lubumbashi, crude refined in Ndola) are in ktonnes. All emissions and their standard deviation values (in parenthesis) are in kg km^2 h^{-1}.

		2019	2020	2021	2022
Kolwezi[a], Katanga[b]	Ore, Waste	-, -	-, -	-, -	-, -
	Grade	4.2, -	4.17, -	2.9, -	-, -
	Copper	84.3, 234.5	114.3, 270.7	121.1, 264.4	-, 220.1
	TROPOMI	0.19 (0.10)	0.24 (0.12)	0.31 (0.15)	0.41 (0.17)
	Background	0.23 (0.08)	0.23 (0.10)	0.22 (0.10)	0.26 (0.10)
	Inventory	0.03	0.03	0.03	-
Sentinel[c]	Ore, Waste	50263, 92826	60098, 97970	57380, 102445	56219, 95335
	Grade	0.5	0.49	0.47	0.46
	Copper	220.006	251.216	232.688	242.451
	TROPOMI	0.23 (0.11)	0.27 (0.12)	0.33 (0.10)	0.26 (0.11)
	Background	0.20 (0.07)	0.22 (0.08)	0.21 (0.07)	0.24 (0.07)
	Inventory	0.01	0.01	0.01	-
Lumwana[d]	Ore, Waste	23230, 62837	26880, 73480	33510, 65499	20277, 78063
	Grade	0.47	0.52	0.46	0.52
	Copper	107.955	125.191	109.769	121.109
	TROPOMI	0.20 (0.06)	0.29 (0.08)	0.27 (0.09)	0.21 (0.06)
	Background	0.21 (0.07)	0.22 (0.07)	0.21 (0.07)	0.24 (0.07)
	Inventory	0.04	0.04	0.04	-
Kansanshi[c]	Ore, Waste	36325, 52768	34423, 61972	35142, 69758	28205, 75878
	Grade	0.89, 1.05, 1.12	0.83, 1.00, 0.93	0.88, 0.96, 0.72	0.71, 0.63, 0.57
	Copper	232.243	221.487	202.159	146.282
	TROPOMI	0.22 (0.07)	0.31 (0.09)	0.33 (0.11)	0.28 (0.10)
	Background	0.22 (0.07)	0.23 (0.08)	0.22 (0.07)	0.24 (0.07)
	Inventory	0.08	0.08	0.08	-
Lubumbashi[e]	Throughput	-	-	255.229	-
	TROPOMI	0.23 (0.10)	0.23 (0.10)	0.30 (0.16)	0.28 (0.17)
	Background	0.25 (0.08)	0.26 (0.08)	0.25 (0.08)	0.26 (0.08)
	Inventory	0.25	0.26	0.26	-
Ndola[f]	Throughput	700.277	372.384	56.672	0[g]
	TROPOMI	0.58 (0.30)	0.32 (0.10)	0.26 (0.13)	0.17 (0.10)
	Background	0.20 (0.09)	0.21 (0.09)	0.21 (0.08)	0.23 (0.08)
	Inventory	0.22	0.22	0.22	-

[a]Zijin (2023). [b]Glencore (2023). [c]First Quantum (2023a). [d]Barrick (2023). [e]STL (2023). [f]Mwila et al. (2022). [g]Inactive.

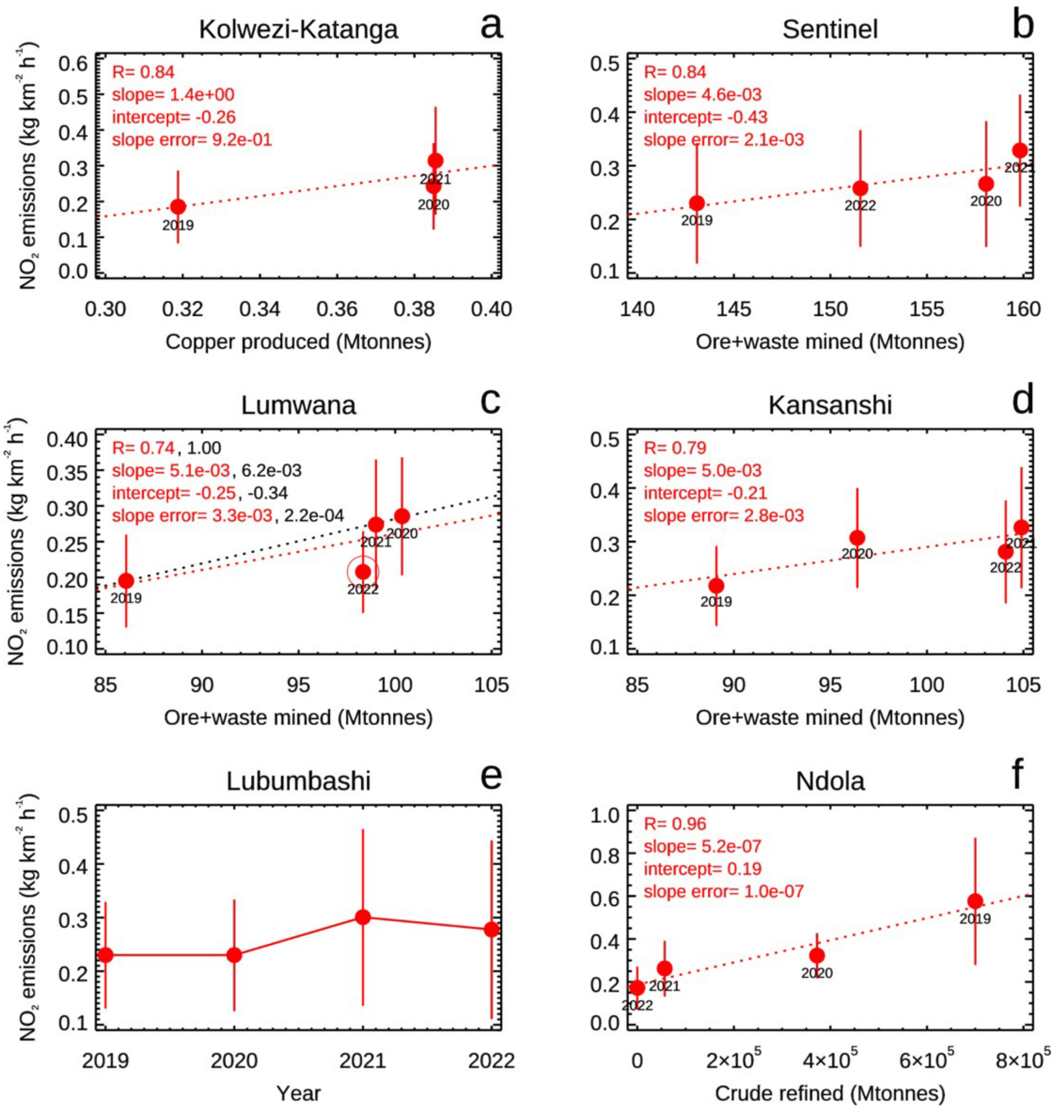

Figure 2. TROPOMI-derived, background-removed NO_2 emissions and their standard deviation versus production, except (e), where production data is unavailable. (c) Statistical values and fit line in black exclude 2022 values; see text for details.

bashi are higher than those from Mbuji-Mayi by 90 %, even though the population of the former is lower by 2 %. Similarly, while its population is lower by 27 %, emissions from Ndola surpass those from Kitwe by 40-80 %, depending on the year, and display inter-annual variations which do not correlate with changes in population. These findings are consistent with our hypothesis that emissions from Lubumbashi and Ndola are not the result of urban activity alone. We researched other possible origins for the excess emissions observed at these two point sources. We hypothesize that Lubumbashi's high NO_2 emissions are due to reprocessing of the Lubumbashi slag heap: a 14.5 x 10^6 tonne hill of mining residue located inside the city, resulting from metallurgical activity between 1924 and 1992 (Peˇsa, 2022). Copper, cobalt, and zinc are extracted from the slag heap by La Société Congolaise du Terril de Lubumbashi (2000-present). Reports from the local press attest to the pollution resulting from the operation (Africa Intelligence, 2021). Figure 2.e shows annual background-removed TROPOMI-derived NO_2 emissions; because production data is incomplete (STL, 2023; The Carter Center, 2023), emissions and mining-related activity cannot be compared in this case. The most plausible emissions source in Ndola is the INDENI petroleum refinery plant, located inside the city. Inactive since late 2021, its declining production values (Mwila et al., 2022) match well the TROPOMI-derived NO_2 emissions (R = 0.96, Fig. 2.f).

The six Copperbelt NO_2 emission point sources do not coincide with SO_2 enhancements, as shown by the map of mean TROPOMI SO_2 VCD values for the period between January 2019 and July 2022 (Fig. 3). The map shows SO_2 enhancements elsewhere: collocated with the Hwange coal power plant (Zimbawe), the Selous smelter (Zimbawe), and the Chingola and Mufulira smelters (Zambia).

Anthropogenic emissions from the inventory were compared to TROPOMI-derived emissions from our six point sources. Monthly inventory emissions from the following sectors were aggregated: power generation, industrial processes (including mining), road and non-road transportation, residential, fugitive fuel emissions, solvents application and production, and solid waste and wastewater handling. Emissions from the agriculture livestock, agriculture soils, and agriculture waste burning sectors would be part of the background over mines and cities and, thus, were excluded. Aggregated inventory emissions were converted to NO_2 ($NO_2 = NO_x / 1.32$; Beirle et al. (2019), Dix et al. (2022)). The highest inventory value among the nine data points coinciding spatially with each point source was selected; annual inventory means were calculated and compared to their background-removed TROPOMI-derived emissions counterparts (Table 1 and Fig. S5). The inventory underpredicts mine emissions by 61-96 %, generally overpredicts city emissions, and does not identify the annual trends in both TROPOMI-derived emissions and mine production.

5 Discussion

We have shown that NO_2 from copper/cobalt mining and other industrial activities can be identified and emissions quantified from satellite, even in the presence of high background values from biomass burning, soils, and lightening. Furthermore, we have demonstrated strong positive correlations between annual TROPOMI-derived NO_2 emissions and mine production/refinery throughput. These correlations are mine-dependent and cannot be extrapolated from mine to mine; differences in ore grades and equipment fuel efficiency are probably the main causes. As an example, lower-than-expected 2022 emissions from Lumwana, which reduced R from 1.00 (for 2019-2021) to 0.74 (for 2019-2022) (Fig. 2.c), can be traced to a new fleet of trucks and shovels commissioned in 2021 (Barrick, 2023) and in operation during 2022 (Lusaka Times, 2022).

As a reference, 2019 background-removed TROPOMI-derived NO_2 emissions from Ndola (0.044kg/s , after accounting for point source area) are equivalent to NO_2 emissions from the Miami Fort or the Intermountain coal power plants, both among the ten

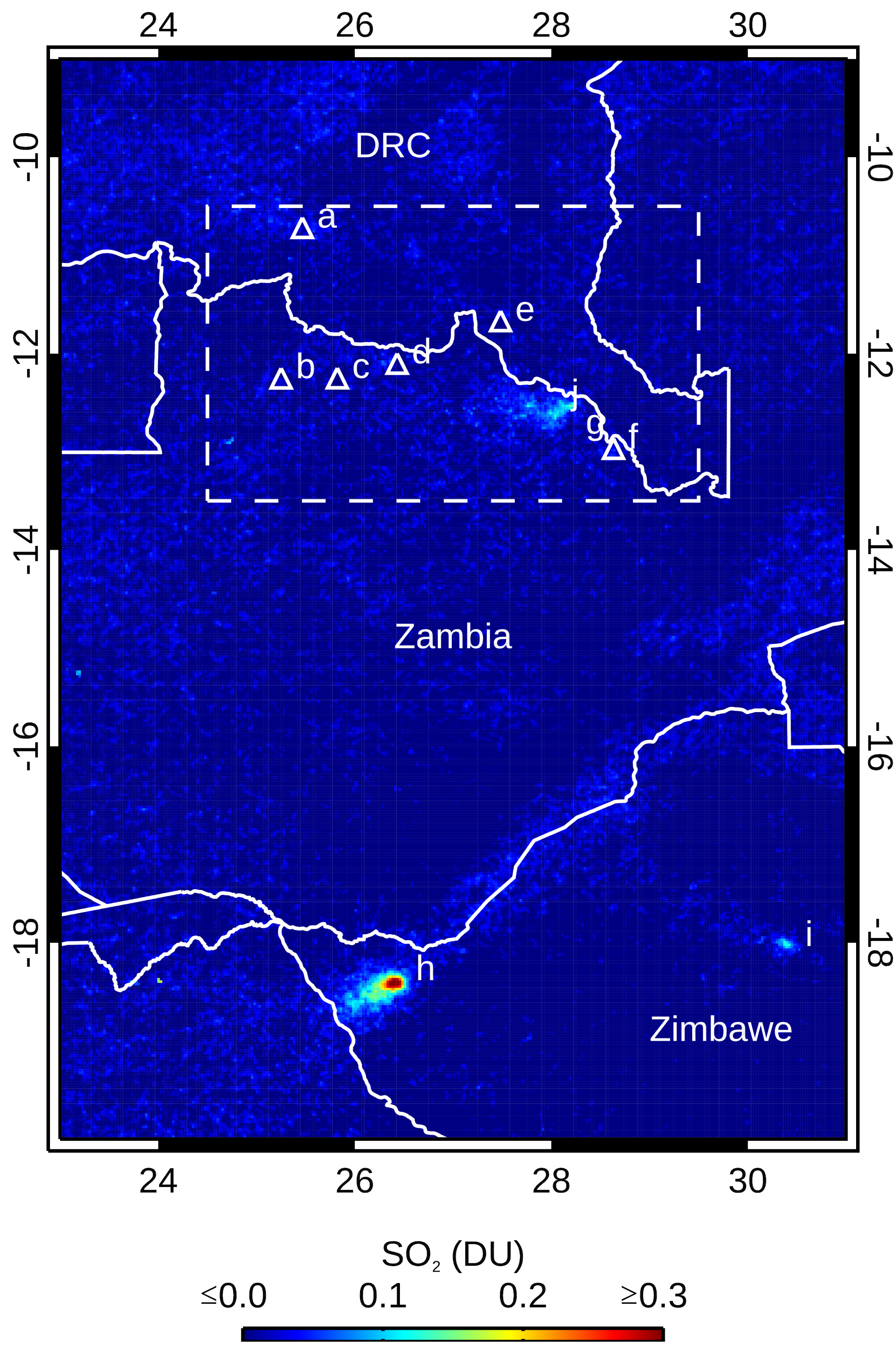

Figure 3. Mean TROPOMI-COBRA SO_2 VCD for January 2019 - July 2022. White triangles show the Copperbelt NO_2 emission point sources analyzed. (a) Kolwezi-Katanga. (b) Sentinel. (c) Lumwana. (d) Kansanshi. (e) Lubumbashi. (f) Ndola. (g) Kitwe. (h) Hwange coal power plant. (i) Selous smelter. (j) Chingola-Mufulira smelters. White lines show country boundaries. Dashed white lines show Copperbelt study area.

largest NO_x emitters in the USA that year (Beirle et al., 2021). Our results demonstrate that the impact of mining/oil refining on local air quality can be quantified using satellite data; this is particularly important for African regions where mining and other industrial activities proliferate without sufficient air quality monitoring.

We have analyzed the point sources with the highest mean annual TROPOMI-derived emissions in the Copperbelt; our maps do, however, show a string of NO_2 enhancements along the Ndola-Lubumbashi-Kolwezi corridor (Fig. 1) where relatively smaller copper/cobalt mining operations, both industrial and artisanal, exist. Future work should explore the detection limits of this method by analyzing some of these other NO_2 enhancements.

Ground emission measurements were unavailable; thus, we compared background-removed TROPOMI-derived NO_2 emissions to inventory data. Inventory values are lower (higher) for mines (cities) than their TROPOMI counterparts and do not capture the annual trends revealed by TROPOMI. The remoteness of the region, lack of field data, and relatively small size of the point sources may explain at least in part these discrepancies. NO_2 emissions derived from satellite measurements could improve the overall magnitude and temporal (seasonal, inter-annual) trends in inventory emissions. They could also be used to refine regional emission factors, which are not well defined for Africa.

We identified SO_2 enhancements coinciding with smelters and a coal power plant elsewhere, but none colocated with our NO_2 point sources (Fig. 3), despite the fact that some of them either include a smelter (Kansanshi, First Quantum (2023a)) or have one nearby (Lualaba, 40 km southeast of Kolwezi; Ivanhoe Mines (2021)). Lack of SO_2 enhancements indicates use of technologies to convert sulfur oxides released from the ore during smelting into sulfuric acid, a commercial byproduct (Hocking, 2005; Ialongo et al., 2018). The use of such technologies in the Kansanshi and Lualaba smelters has been documented by the mining companies involved (Gray et al., 2020; First Quantum, 2023b; Wang, 2020).

6 Conclusions

Understanding the environmental effects of high-impact minerals extraction and processing is of great relevance (Hund et al., 2020), particularly if the mining-related activities take place in close proximity to -or even inside of- population centers, as is the case in the Copperbelt region. We have shown for the first time that NO_2 emissions from copper and cobalt mining activities can be identified and measured using TROPOMI satellite data, even in the presence of high background NO_2; this is important in the absence of local air quality monitoring. Furthermore, we have shown, also for the first time, a strong positive correlation between TROPOMI-derived NO_2 emissions and mining/oil refining production data. We note that these correlations are mine-dependent and that changes in the mine's environment (ore grade, fuel efficiency) will affect such correlations, as observed in Lumwana. The lack of SO_2 enhancements colocated with our NO_2 point sources (enhancements identified, though, in power plants and smelters nearby) is consistent with SO_2 capture and transformation into sulfuric acid, which is then used in mining-related processes or commercialized.

Because the NO_2 emissions analyzed result from the combustion of fossil fuels by machinery (e.g., trucks, crushers, generators) used extensively in mining operations, these results are relevant to mining in general, regardless of the resource mined. They are also relevant to oil refineries, as shown in Ndola. We hypothesize that our findings apply to fossil-fuel intensive industries in general.

Our results show that NO_2 trend analysis can be used to predict mine production and refinery throughput before companies release their reports or in lieu of these reports in case of non-publicly traded companies, which are not required to publish their activity data. Insufficient emissions from mines claiming high production may be indicative of production from a different source. Thus, this method may be useful for improving traceability of minerals extracted in conflict areas and smuggled into the global supply chain despite existing traceability and tagging schemes, an issue highlighted in the most recent releases of the United Nations Yearbook (United Nations, 2019, 2022).

Open Research Section

Atmospheric data available as follows. TROPOMI NO_2 data (L2__NO2_) are publicly available via the ESA's S5P Pre-Ops interface (https://scihub.copernicus.eu/) using the credentials given there. TROPOMI SO2 COBRA data: https://distributions.aeronomie.be/?menu=68c9f961bc294141c215e3d64a6ae282#. ERA5 data: https://cds.climate.copernicus.eu/cdsapphttps://cds.climate.copernicus.eu/cdsapp#!/dataset/reanalysis-era5-single-levels-monthly-means?tab=form (hourly data on single levels) and https://cds.climate.copernicus.eu/cdsapp#!/dataset/reanalysis-era5-pressure-levels?tab=form (hourly data on pressure levels). CAMS-GLOB-ANT inventory data are publicly available via the https://eccad3.sedoo.fr/ interface following the instructions given there to create a free access account. Mining production data available from mining company reports as follows. First Quantum Minerals Ltd. (Sentinel, Kansanshi): https://s24.q4cdn.com/821689673/files/doc_downloads/2019-annual-report/First_Quantum_AR_2019.pdf (2019), https://s24.q4cdn.com/821689673/files/doc_downloads/2020-annual-report/First_Quantum_2020_Annual_Report.pdf (2020), https://www.firstquantum-2021-annual-report.com/_files/ugd/acdda3_c51ed134aa184e259d61a629344f98e7.pdf (2021), https://www.first-quantum.com/files/doc_downloads/2022-annual-report/First-Quantum-2022- AR-online.pdf (2022). Barrick Gold Corporation (Lumwana): https://s25.q4cdn.com/322814910/files/doc_financial/annual_reports/2019/Barrick-Annual- Report-2019.pdf (2019), https://s25.q4cdn.com/322814910/files/doc_financial/annual_reports/2020/Barrick-Annual- Report-2020.pdf (2020), https://s25.q4cdn.com/322814910/files/doc_financial/annual_reports/2021/Barrick_Annual_Report_2021.pdf (2021), https://s25.q4cdn.com/322814910/files/doc_financial/annual_reports/2022/Barrick_Annual_Report_2022.pdf (2022). Zijing Mining (Kolwezi): https://www.zijinmining.com/upload/file/2020/09/14/9c97a89f8e9c4c59a13f2404f3bb1096.pdf (2019), https://www.zijinmining.com/upload/file/2021/06/09/538a46cc4831452e97b30cae55c9cf97.pdf (2020), https://www.zijinmining.com/upload/file/2022/06/20/771c971d76154257882f58ed03643c07.pdf (2021; no 2022 annual report available at the time of writing). Glencore (Katanga): https://www.glencore.com/.rest/api/v1/documents/5a08fe1942f92df7f2301ac3681e23aa/glen- 2019-annual-report-interactive.pdf?download=true (2019), https://www.glencore.com/.rest/api/v1/documents/3505497f3cb94b24f0c79f5ba32b293b/Glencore_AR20_Interactive+%281%29.pdf?download=true (2020), https://www.glencore.com/.rest/api/v1/documents/ce4fec31fc81d6049d076b15db35d45d/GLEN-

2021-annual-report-.pdf?download=true (2021), https://www.glencore.com/.rest/api/v1/documents/ded10fa92974aa388a43aa9f86f483e9/GLEN-2022-Annual-Report.pdf (2022).

ERA5 data are produced by C3S and CAMS. Contains modified information from C3S and CAMS [2019-2021]. Neither the European Commission nor ECMWF is responsible for any use that may be made of the Copernicus information data contained in this study.

Acknowledgments

SMA thanks William Atkinson for sharing his deep knowledge of minerals and mining; Carol Atkinson for her insights and inspiring curiosity; Louisa Emmons for advice regarding models; David Edwards and Bill Randel for helpful NCAR in-house comments.

This material is based upon work supported by the National Center for Atmospheric Research, which is a major facility sponsored by the National Science Foundation under Cooperative Agreement No. 1852977.

References

Africa Intelligence. (2021). *Lubumbashi slag heap locals fume over pollution.* Retrieved from https://www.africaintelligence.com/central-africa/2021/05/25/lubumbashi-slag-heap-locals-fume-over-pollution,109668540-art (last access: 19 February 2023)

Allen, M. (2021). *Mining Energy Consumption 2021* (Tech. Rep.). ENGECO Pte. Ltd. Retrieved from https://www.ceecthefuture.org/resources/mining-energy-consumption-2021 (last access: 21 February 2023)

Atibu, E. K., Devarajan, N., Laffite, A., Giuliani, G., Salumu, J. A., Muteb, R. C., ... Pore, J. (2016). Assessment of trace metal and rare earth elements contamination in rivers around abandoned and active mine areas. The case of Lubumbashi River and Tshamilemba Canal, Katanga, Democratic Republic of the Congo. *CHEMIE DER ERDE-GEOCHEMISTRY*, *76*(3), 353-362. doi: 10.1016/j.chemer.2016.08.004

Barrick. (2023). *Annual reports.* Retrieved from https://www.barrick.com/English/investors/default.aspx (last access: 08 February 2023)

Beirle, S., Boersma, K. F., Platt, U., Lawrence, M. G., & Wagner, T. (2011). Megacity emissions and lifetimes of nitrogen oxides probed from space. *SCIENCE*, *333*(6050), 1737-1739. doi: 10.1126/science.1207824

Beirle, S., Borger, C., Doerner, S., Eskes, H., Kumar, V., de Laat, A., & Wagner, T.

(2021). Catalog of NO_x emissions from point sources as derived from the divergence of the NO_2 flux for TROPOMI. *EARTH SYSTEM SCIENCE DATA*, *13*(6), 2995-3012. doi: 10.5194/essd-13-2995-2021

Beirle, S., Borger, C., Drner, S., Li, A., Hu, Z., Liu, F., . . . Wagner, T. (2019). Pinpointing nitrogen oxide emissions from space. *Science Advances*, *5*, eaax9800. doi: 10.1126/sciadv.aax9800

BIRA-IASB. (2021). *Global map of nitrogen dioxide (NO_2).* Retrieved from https://uv-vis.aeronomie.be/data/tropomi_posters/posterTROPOMI_NO2_2018_2020.pdf (last access: 7 April 2023)

Carn, S. A., Krueger, A. J., Krotkov, N. A., Yang, K., & Levelt, P. F. (2007). Sulfur dioxide emissions from Peruvian copper smelters detected by the Ozone Monitoring Instrument. *GEOPHYSICAL RESEARCH LETTERS*, *34*(9). doi: 10.1029/2006GL029020

de Foy, B., & Schauer, J. J. (2022). An improved understanding of NO_x emissions in South Asian megacities using TROPOMI NO_2 retrievals. *ENVIRONMENTAL RESEARCH LETTERS*, *17*(2). doi: 10.1088/1748-9326/ac48b4

Dix, B., Francoeur, C., Li, M., Serrano-Calvo, R., Levelt, P. F., Veefkind, J. P., . . . de Gouw, J. (2022). Quantifying NO_x Emissions from US Oil and Gas Production Regions Using TROPOMI NO_2. *ACS EARTH AND SPACE CHEMISTRY*, *6*(2), 403-414. doi: 10.1021/acsearthspacechem.1c00387

Eskes, H., van Geffen, J., Boersma, F., Eichmann, K.-U., Apituley, A., Pedergnana, M., . . . Loyola, D. (2022). *Sentinel-5 precursor/TROPOMI Level 2 Product User Manual Nitrogen dioxide* (Tech. Rep. Nos. 2.4.0, 2021-07-11). Netherlands Institute for Space Research (SRON).

Eskes, H. J., & Eichmann, K.-U. (2021). *S5P mission performance centre nitrogen dioxide (L2 NO_2) readme* (Tech. Rep. Nos. 2.1, 2021-11-17). Netherlands Institute for Space Research (SRON).

Fioletov, V., McLinden, C. A., Griffin, D., Abboud, I., Krotkov, N., Leonard, P. J. T., . . . Carn, S. (2023). Version 2 of the global catalogue of large anthropogenic and volcanic SO_2 sources and emissions derived from satellite measurements. *EARTH SYSTEM SCIENCE DATA*, *15*(1), 75-93. doi: 10.5194/essd-15-75-2023

Fioletov, V., Mclinden, C. A., Griffin, D., Theys, N., Loyola, D. G., Hedelt, P., . . . Li, C. (2020). Anthropogenic and volcanic point source SO_2 emissions derived from TROPOMI on board Sentinel-5 Precursor: first results. *ATMOSPHERIC CHEMISTRY AND PHYSICS*, *20*(9), 5591-5607. doi: 10.5194/acp-20-5591-2020

Fioletov, V. E., McLinden, C. A., Krotkov, N., Yang, K., Loyola, D. G., Valks, P., . . . Martin, R. V. (2013). Application of OMI, SCIAMACHY, and GOME-2 satellite SO_2 retrievals for detection of large emission sources. *JOURNAL OF GEOPHYSICAL RESEARCH-ATMOSPHERES*, *118*(19), 11399-11418. doi: 10.1002/jgrd.50826

First Quantum. (2023a). *Annual reports.* Retrieved from https://www.first-quantum.com/English/investors/financial-information/default.aspx (last access: 08 February 2023)

First Quantum. (2023b). *Kansanshi: smelter.* Retrieved from https://www.first-quantum.com/English/our-operations/default.aspx#module-operation--kansanshi (last access: 24 March 2023)

Glencore. (2023). *Annual reports.* Retrieved from https://www.glencore.com/publications (last access: 08 February 2023)

Goldberg, D. L., Lu, Z., Streets, D. G., de Foy, B., Griffin, D., McLinden, C. A., . . . Eskes, H. (2019). Enhanced Capabilities of TROPOMI NO_2: Estimating NO_x from North American Cities and Power Plants. *ENVIRONMENTAL SCIENCE & TECHNOLOGY*, *53*(21), 12594-12601. doi: 10.1021/acs.est.9b04488

Granier, C., S. Darras, H. Denier van der Gon, J. Doubalova, N. Elguindi, B. Galle, M. Gauss, M. Guevara, J.-P. Jalkanen, J. Kuenen, C. Liousse, B. Quack, D. Simpson, K. Sindelarova, The Copernicus Atmosphere Monitoring Service global and regional emissions, Copernicus Atmosphere Monitoring Service (CAMS) report, doi:10.24380/d0bn-kx16, 2019

Gray, D., Lawlor, M., & Briggs, A. (2020). *Kansanshi Operations, North West Province, Zambia, NI 43-101 Technical Report, June 2020* (Tech. Rep.). First Quantum Minerals Ltd.

Gulley, A. L. (2022). One hundred years of cobalt production in the Democratic Republic of the Congo. *Resources Policy*, *79*. doi: 10.1016/j.resourpol.2022.103007

Hersbach, H., Bell, B., Berrisford, P., Hirahara, S., Horanyi, A., Munoz-Sabater, J., . . . Thepaut, J.-N. (2020). The ERA5 global reanalysis. *QUARTERLY JOURNAL OF THE ROYAL METEOROLOGICAL SOCIETY*, *146*(730), 1999-2049. doi: 10.1002/qj.3803

Hocking, M. B. (2005). Ore Enrichment and Smelting of Copper. In M. B. Hocking (Ed.), *Handbook of Chemical Technology and Pollution Control* (Third ed., p. 391-420). San Diego: Academic Press. doi: 10.1016/B978-012088796-5/50016-8

Hund, K., LaPorta, D., Fabregas, T., Laing, T., & Drexhage, J. (2020). *Minerals for climate action: The mineral intensity of the clean energy transition.* The World Bank. Retrieved from https://pubdocs.worldbank.org/en/961711588875536384/Minerals-for-Climate-Action-The-Mineral-Intensity-of-the-Clean-Energy-Transition.pdf

Ialongo, I., Fioletov, V., McLinden, C., Jafs, M., Krotkov, N., Li, C., & Tamminen, J. (2018). Application of satellite-based sulfur dioxide observations to support the cleantech sector: Detecting emission reduction from copper smelters. *Environmental Technology & Innovation*, *12*, 172-179. doi: 10.1016/j.eti.2018.08.006

Ivanhoe Mines. (2021). *Agreement signed with nearby Lualaba Copper Smelter to produce 99% blister copper in the Democratic Republic of Congo.* Retrieved from http://www.sulphuric-acid.com/sulphuric-acid-on-the-web/acid\%20plants/Lualaba-Copper-Smelter.htm (last access: 22 February 2023)

Kayembe-Kitenge, T., Lubala, T. K., Obadia, P. M., Chimusa, P. K., Nawej, C. K., Nkulu, C. B. L., . . . Nemery, B. (2019). Holoprosencephaly: A case series from an area with high mining-related pollution. *BIRTH DEFECTS RESEARCH*, *111*(19), 1561-1563. doi: 10.1002/bdr2.1583

Krueger, A. (1983). SIGHTING OF EL-CHICHON SULFUR-DIOXIDE CLOUDS WITH THE NIMBUS-7 TOTAL OZONE MAPPING SPECTROMETER. *SCIENCE*, *220*(4604), 1377-1379. doi: 10.1126/science.220.4604.1377

Labzovskii, L. D., Belikov, D. A., & Damiani, A. (2022). Spaceborne NO_2 observations are sensitive to coal mining and processing in the largest coal basin of Russia. *SCIENTIFIC REPORTS*, *12*(1). doi: 10.1038/s41598-022-16850-8

Leue, C., Wenig, M., Wagner, T., Klimm, O., Platt, U., & Jahne, B. (2001). Quantitative analysis of NO_x emissions from Global Ozone Monitoring Experiment satellite image sequences. *JOURNAL OF GEOPHYSICAL RESEARCH-ATMOSPHERES*, *106*(D6), 5493-5505. (2nd AGU Chapman Conference on Water Vapor in the Climate System, POTOMAC, MD, OCT 12-15, 1999) doi: 10.1029/2000JD900572

Lusaka Times. (2022). *Barrick hoping to extend Lumwana mine to 2042.* Retrieved from https://www.lusakatimes.com/2022/10/31/barrick-hoping-to-extend-lumwana-mine-to-2042/ (last access: 28 February 2023)

Mwila, A. M., et al. (Eds.). (2022). *2021 Energy Sector Report* (Tech. Rep.). Energy Regulation Board, Zambia.

Mwitwa, J., German, L., Muimba-Kankolongo, A., & Puntodewo, A. (2012). Governance and sustainability challenges in landscapes shaped by mining:

Mining-forestry linkages and impacts in the Copper Belt of Zambia and the DR Congo. *FOREST POLICY AND ECONOMICS*, *25*, 19-30. doi: 10.1016/j.forpol.2012.08.001

Myhre, G., Shindell, D., Bron, F.-M., Collins, W., Fuglestvedt, J., Huang, J., . . . Zhang, H. (2013). Anthropogenic and natural radiative forcing. In T. F. Stocker et al. (Eds.), *Climate Change 2013: The Physical Science Basis. Contribution of Working Group I to the Fifth Assessment Report of the Intergovernmental Panel on Climate Change* (pp. 659–740). Cambridge, UK: Cambridge University Press. doi: 10.1017/CBO9781107415324.018

Pe˘sa, I. (2022). Mining, Waste and Environmental Thought on the Central African Copperbelt, 1950-2000. *ENVIRONMENT AND HISTORY*, *28*(2), 259-284. doi: 10.3197/096734019X15755402985703

Pommier, M. (2022). Estimations of NO_x emissions, NO_2 lifetime and their temporal variation over three British urbanised regions in 2019 using TROPOMI NO_2 observations. *ENVIRONMENTAL SCIENCE-ATMOSPHERES*. doi: 10.1039/d2ea00086e

Population Stat. (2023). *World statistical data.* Retrieved from https://populationstat.com/ (last access: 18 February 2023)

Richter, A., Begoin, M., Hilboll, A., & Burrows, J. P. (2011). An improved NO_2 retrieval for the GOME-2 satellite instrument. *Atmospheric Measurement Techniques*, *4*(6), 1147–1159. Retrieved from https://amt.copernicus.org/articles/4/1147/2011/ doi: 10.5194/amt-4-1147-2011

Richter, A., Burrows, J., Nuss, H., Granier, C., & Niemeier, U. (2005). Increase in tropospheric nitrogen dioxide over China observed from space. *NATURE*, *437*(7055), 129-132. doi: 10.1038/nature04092

Shedd, K. B. (2022). *Cobalt. In: 2022 Mineral Commodity Summaries.* (Tech. Rep.). U.S. Geological Survey.

STL. (2023). *Statistiques de production.* Retrieved from http://www.stlgcm.com/ (last access: 19 February 2023)

The Carter Center. (2023). *Mining royalty statistics for the province of H-Katanga / Cumulative 2021.* Retrieved from https://congomines.org/reports/ (last access: 18 February 2023)

Theys, N. (2022). *S5P COBRA Sulphur Dioxide (L2 SO2CBR) Readme* (Tech. Rep. Nos. 1.0.0, 2022-09-14). Royal Belgian Institute for Space Aeronomy (BIRA-IASB).

Theys, N., Fioletov, V., Li, C., De Smedt, I., Lerot, C., McLinden, C., . . . Van Roozendael, M. (2021). A sulfur dioxide Covariance-Based Retrieval Algorithm (COBRA): application to TROPOMI reveals new emission sources. *ATMOSPHERIC CHEMISTRY AND PHYSICS*, *21*(22), 16727-16744. doi: 10.5194/acp-21-16727-2021

United Nations. (2019). (O. F. Summerell et al., Eds.). New York, NY, USA: United Nations Department of Global Communications. Retrieved from https://www.unmultimedia.org/searchers/yearbook/page_un2.jsp?volume=2014&page=1

United Nations. (2022). New York, NY, USA: United Nations Department of Global Communications. Retrieved from https://www.un.org/en/yearbook/prepress

U.S. Bureau of Mines (Ed.). (1993). *1990 Minerals Yearbook: Mineral Industries of Africa* (Tech. Rep.). U.S. Bureau of Mines.

Van Brusselen, D., Kayembe-Kitenge, T., Mbuyi-Musanzayi, S., Kasole, T. L., Ngombe, L. K., Obadia, P. M., . . . Nemery, B. (2020). Metal mining and birth defects: a case-control study in Lubumbashi, Democratic Republic of the Congo. *LANCET PLANETARY HEALTH*, *4*(4), E158-E167.

van Geffen, J., Boersma, K. F., Eskesl, H., Sneep, M., ter Linden, M., Zara, M., & Veefkind, J. P. (2020). S5P TROPOMI NO_2 slant column retrieval: method, stability, uncertainties and comparisons with OMI. *ATMOSPHERIC MEASUREMENT TECHNIQUES*, *13*(3), 1315-1335. doi: 10.5194/amt-13-1315-2020

Veefkind, J. P., Aben, I., McMullan, K., Forster, H., de Vries, J., Otter, G., . . . Levelt, P. F. (2012). TROPOMI on the ESA Sentinel-5 Precursor: A GMES mission for global observations of the atmospheric composition for climate, air quality and ozone layer applications [Article]. *Remote Sensing of Environment*, *120*(SI), 70-83. doi: {10.1016/j.rse.2011.09.027}

Wang, R. (2020). *CNMC-invested and constructed mining, copper smelting projects go into production.* Retrieved from http://en.sasac.gov.cn/2020/01/22/c_12660.htm (last access: 24 March 2023)

World Health Organization. (2021). *WHO global air quality guidelines: particulate matter (PM2.5 and PM10), ozone, nitrogen dioxide, sulfur dioxide and carbon monoxide* [Publications]. World Health Organization.

Zhang, Y., Li, C., Krotkov, N. A., Joiner, J., Fioletov, V., & McLinden, C. (2017). Continuation of long-term global SO_2 pollution monitoring from OMI to OMPS. *ATMOSPHERIC MEASUREMENT TECHNIQUES*, *10*(4). doi: 10.5194/amt-10-1495-2017

Zijin. (2023). *Annual reports.* Retrieved from https://www.zijinmining.com/investors/Annual-Reports.jsp (last access: 08 February 2023)

TROPOMI NO_2 emissions from mining and other industrial activities in the Copperbelt (DRC and Zambia)

—

SUPPLEMENT

S. Martínez-Alonso[1], P. Veefkind[2,3], B. Dix[4], B. Gaubert[1], N. Theys[5], C. Granier[4,6,7], A. Soulié[6], S. Darras[8], H. Eskes[2], W. Tang[1], H. Worden[1], J. de Gouw[4,9], and P. Levelt[1,2,3]

[1]ACOM-NCAR, Boulder, Colorado, USA
[2]KNMI, De Bilt, The Netherlands
[3]Department of Civil Engineering and Geosciences, Technical University of Delft, Delft, The Netherlands
[4]CIRES, University of Colorado, Boulder, Colorado, USA
[5]BIRA-IASB, Brussels, Belgium
[6]Laboratoire dAérologie, CNRS, University of Toulouse UPS, Toulouse, France
[7]NOAA-CSL, Boulder, Colorado, USA
[8]Observatoire Midi-Pyrénées, Toulouse, France
[9]Department of Chemistry, University of Colorado Boulder, Boulder, Colorado, USA

S1 Effect on TROPOMI Emissions of ERA5 Wind Data Uncertainty

We have quantified the error in TROPOMI-derived NO_2 raw emissions (i.e., emissions before background removal) due to uncertainties in the ERA5 wind data. Wind uncertainty was estimated from the spread of the 10-member ensemble of ERA5 data assimilation. We recalculated annual TROPOMI emissions for 2020 over the Copperbelt study area (-10.5^{o}N to -13.5^{o}N, 24.5^{o}E to 29.5^{o}E) after perturbing the wind data by first adding and then subtracting the wind spread. These two sets of perturbed results were then compared to unperturbed TROPOMI emissions for the same year and region. Results are shown in Fig. S1 and summarized in Table S1. Differences between unperturbed and perturbed emissions are in all cases below 4 %.

S2 Annual TROPOMI Maps of VCD and Emissions

Annual maps of TROPOMI NO_2 VCD (Vertical Column Density) were produced for the years between 2019 and 2022 from daily TROPOMI VCD data (Fig. S2). The maps show six distinct emission point sources which coincide with copper or copper-cobalt mines (points a to d) and cities (points e and f). The VCD maps show inter-annual variability in VCD among the point sources, while background VCD values remain close-to-constant between 2019 and 2021. Background values appear to be higher in 2022.

Figure S3 shows annual maps of raw TROPOMI emissions. These maps show that the magnitude of the emissions released from each point source changes from year to year. Background emissions do not show strong changes.

S3 Are Lubumbashi and Ndola Emissions from Urban Activity Alone?

To test the hypothesis that background-removed TROPOMI emissions from Lubumbashi and Ndola were not produced by urban activity alone, we identified two nearby cities of similar population: Mbuji-Mayi and Kitwe, respectively. We calculated annual

Corresponding author: Sara Martínez-Alonso, sma@ucar.edu

emissions for these two cities using the methodology described in Section 3. Results are summarized in Fig. S4 and Table S2.

Background-removed NO_2 emissions from Lubumbashi are higher than those from Mbuji-Mayi by $\sim$ 90 %, even though the population of the former is lower by $\sim$2 %. Similarly, while its population is lower by $\sim$27 %, emissions from Ndola surpass those from Kitwe by 40-80 %, depending on the year, and display inter-annual variations which do not correlate with changes in population.

These findings are consistent with our hypothesis that emissions from Lubumbashi and Ndola are not the result of urban activity alone.

S4 TROPOMI Emissions versus CAMS-GLOB-ANT v5 Inventory Emissions

We compared CAMS-GLOB-ANT v5 inventory data to TROPOMI-derived NO_2 emissions. Only 2019-2021 inventory data were analyzed because those from 2022 were unavailable at the time of writing. The inventory includes emissions from the following sectors: power generation, industrial processes (including mining), road and non-road transportation, residential, fugitive fuel emissions, solvents application and production, solid waste and wastewater handling, agriculture livestock, agriculture soils, and agriculture waste burning. In order to compare inventory emissions to background-removed TROPOMI emission, we aggregated the emissions from all sectors excluding agriculture livestock, agriculture soils, and agriculture waste burning, since those would be part of the background in mines and cities. We could not compare inventory to raw (i.e., non background-removed) TROPOMI emissions because the inventory does not include other possible background emissions (from wildfires, non-agriculture soils, and lightning).

We aggregated monthly inventory emission values as explained above and converted them from NO_x (the original) into NO_2 ($NO_2 = NO_x / 1.32$; Beirle et al. (2019), Dix et al. (2022)). The highest inventory value among the nine data points coinciding spatially with each point source was selected. The selected inventory values were used to calculate annual means for each point source. Results are presented in Table 1 in the main body of this paper and summarized in Fig. S5.

Emissions from the Copperbelt mines analyzed are not well represented in the inventory (Table 1 and panels a to d in Fig. S5). Inventory values are consistently lower than the TROPOMI emissions (by between 61 and 96 %) and do not show the annual trends identified by TROPOMI. Differences between inventory and TROPOMI emissions for cities (Table 1 and panels e to h in Fig. S5) are between -62 to +1869 %. The inventory overpredicts emissions for Mbuji-Mayi and Kitwe, two cities that we infer have no additional industrial emissions, and most years underpredicts emissions for Lubumbashi and Ndola, where we hypothesize that highly-emittant industrial processes take place.

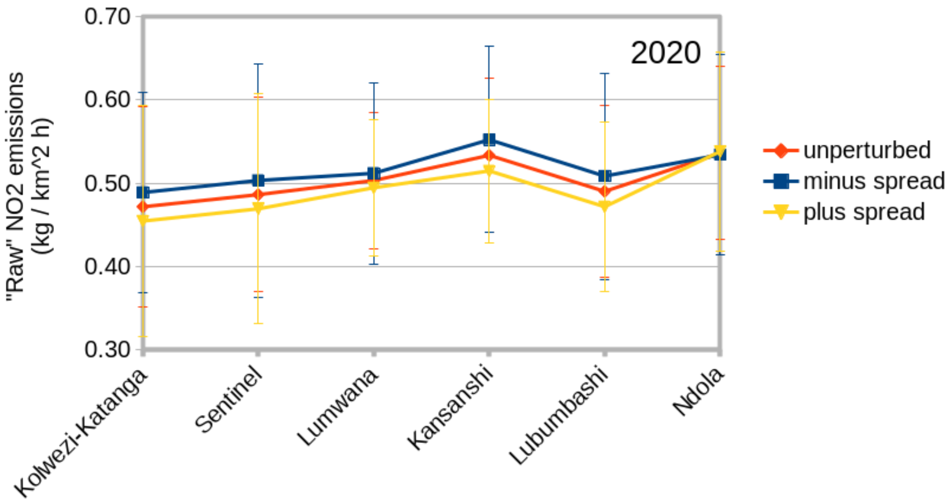

Figure S1. Effect of wind uncertainty (i.e., the spread of the ERA5 10-member wind ensemble) on raw TROPOMI-derived NO_2 emissions for the six point sources analyzed. For 2020 only. Vertical bars show standard deviation of emissions.

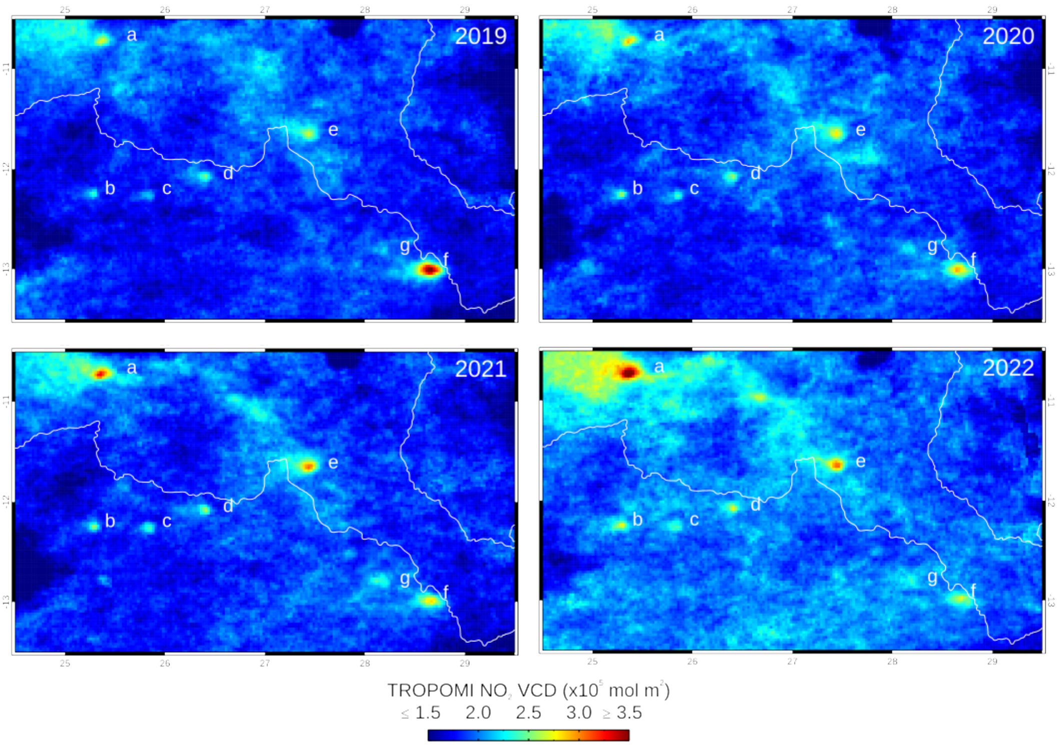

Figure S2. Annual means of TROPOMI NO_2 VCD for the Copperbelt study region. Labels a through f show the six point sources analyzed. a: Kolwezi-Katanga Mines, b: Sentinel Mine, c: Lumwana Mine, d: Kansanshi Mine, e: Lubumbashi City, f: Ndola City. Label g shows location of Kitwe City. White line indicates border between the DRC and Zambia.

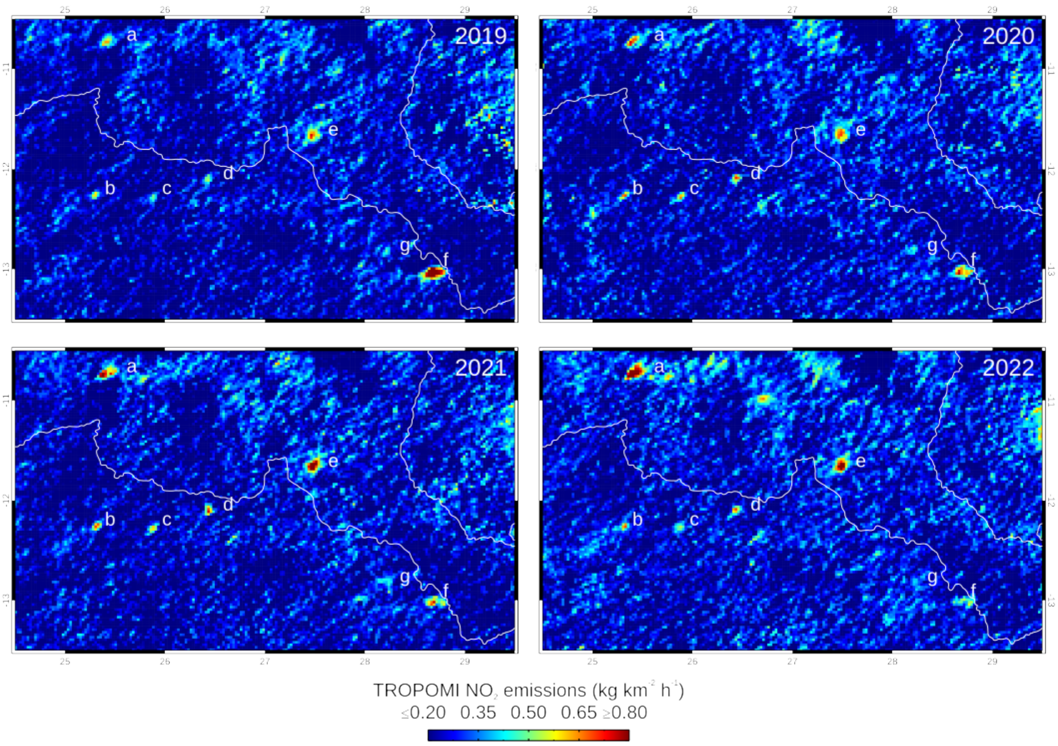

Figure S3. Annual means of TROPOMI-derived NO_2 raw emissions for the Copperbelt study region. Labels a through f show the six point sources analyzed. a: Kolwezi-Katanga Mines, b: Sentinel Mine, c: Lumwana Mine, d: Kansanshi Mine, e: Lubumbashi City, f: Ndola City. Label g shows location of Kitwe City. White lines indicate border between the DRC and Zambia.

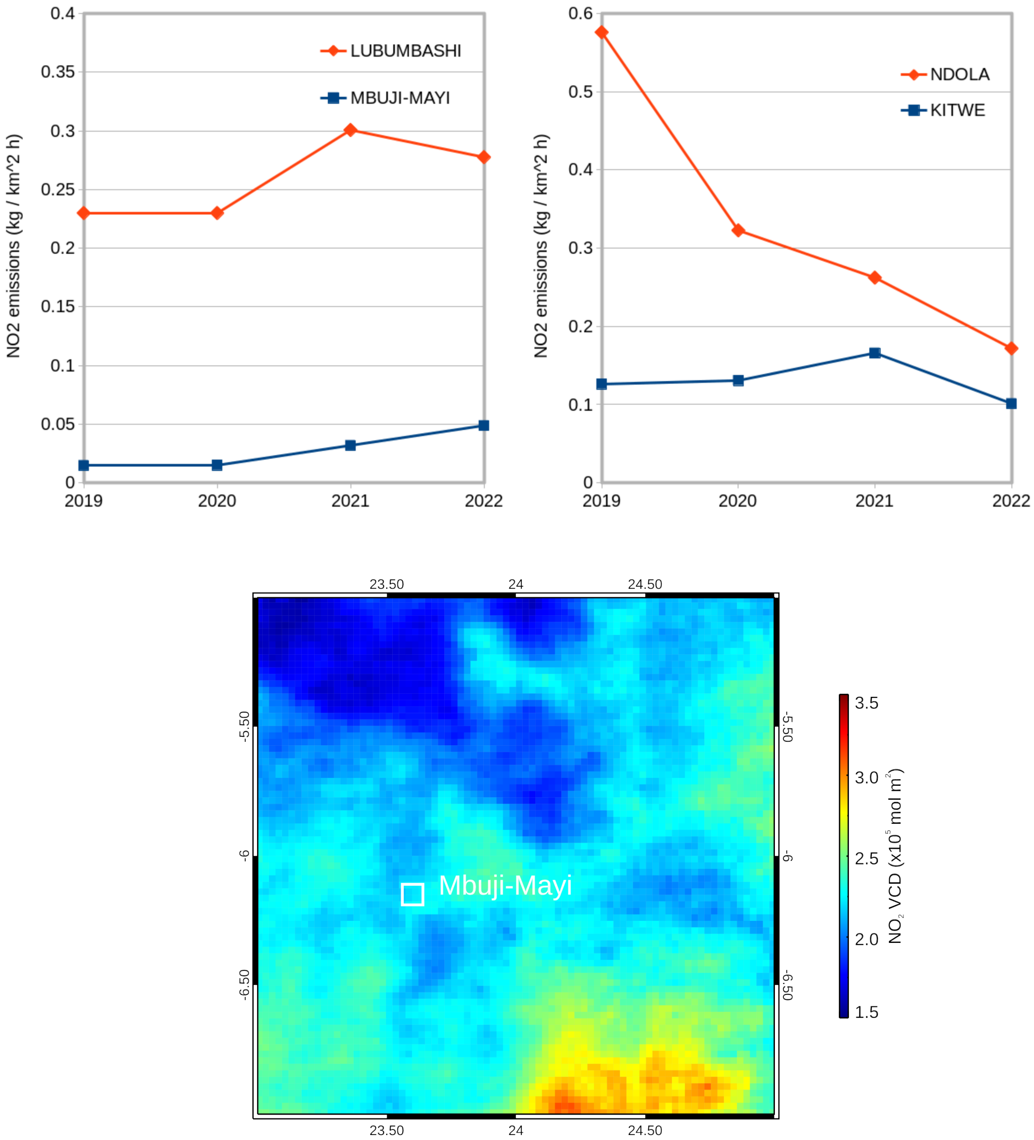

Figure S4. (Top) Time series of annual TROPOMI-derived, background-removed NO_2 emissions for two Copperbelt point sources corresponding to cities (Lubumbashi and Ndola) paired with cities of similar population (Mbuji-Mayi and Kitwe, respectively). The magnitude of the emissions from the two point sources amply surpasses that of the reference cities. The inter-annual trends in emissions from the two point sources cannot be explained by population changes (Table S2). (Bottom) TROPOMI NO_2 VCD shows no plume or enhancement at Mbuji-Mayi which, despite its large population, is a remote and isolated enclave.

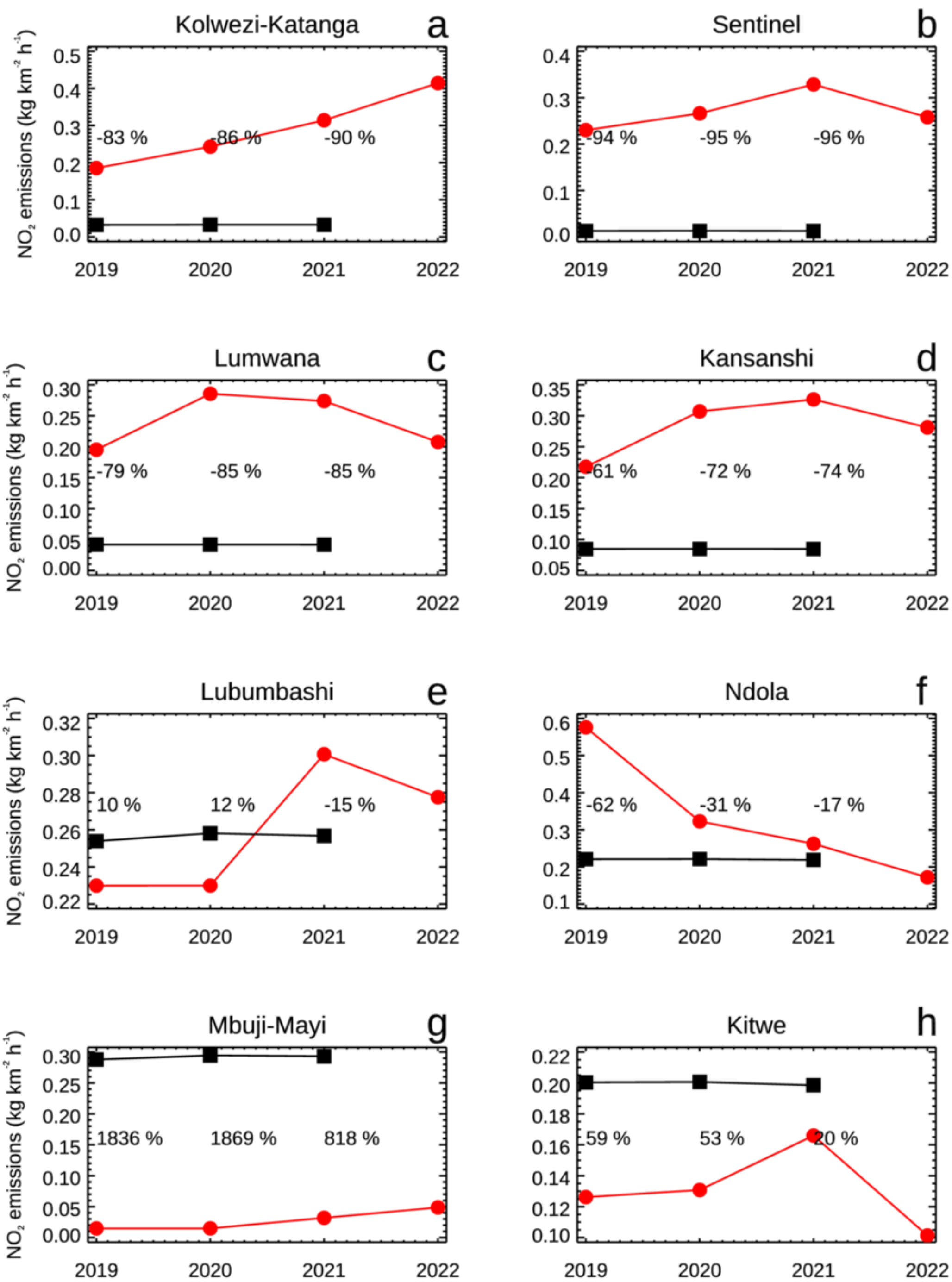

Figure S5. Annual means of NO_2 emissions from TROPOMI (red circles) and the inventory (black squares) for mines (panels a to d) and cities (panels e to h). Percent differences between the two datasets are shown in each panel. TROPOMI emissions have been background-removed. Inventory emissions include all anthropogenic sectors except for agriculture livestock, agriculture soils, and agriculture waste burning, which would be part of the background emissions. Inventory data unavailable for 2022.

Table S1. Effect of wind uncertainty (i.e., ERA5 10 member ensemble spread) on TROPOMI-derived mean NO_2 raw emissions for 2020. Emission values and their standard deviation (in parenthesis) are in kg km^2 h^{-1}.

	Wind - spread	No perturbation	Wind + spread
Kolwezi-Katanga	0.49 (0.12)	0.47 (0.12)	0.45 (0.14)
Sentinel	0.50 (0.14)	0.49 (0.12)	0.47 (0.14)
Lumwana	0.51 (0.11)	0.50 (0.08)	0.49 (0.08)
Kansanshi	0.55 (0.11)	0.53 (0.09)	0.51 (0.09)
Lubumbashi	0.51 (0.12)	0.49 (0.10)	0.47 (0.10)
Ndola	0.53 (0.12)	0.54 (0.10)	0.54 (0.12)

Table S2. TROPOMI-derived NO_2 emission data for two Copperbelt city point sources (Lubumbashi and Ndola) and two additional cities of similar population to each of them (Mbuji-Mayi and Kitwe, respectively). TROPOMI emissions (background-removed, background) as well as their standard deviation values (in parenthesis) are in kg km^2 h^{-1}. Population in million inhabitants.

		2019	2020	2021	2022
	TROPOMI	0.23 (0.10)	0.23 (0.10)	0.30 (0.16)	0.28 (0.17)
Lubumbashi	Background	0.25 (0.08)	0.26 (0.08)	0.25 (0.08)	0.26 (0.08)
	Population	2.377	2.478	2.584	2.695
	TROPOMI	0.01 (0.05)	0.01 (0.04)	0.03 (0.04)	0.05 (0.05)
Mbuji-Mayi	Background	0.28 (0.06)	0.29 (0.06)	0.30 (0.06)	0.32 (0.07)
	Population	2.413	2.525	2.643	2.765
	TROPOMI	0.58 (0.30)	0.32 (0.10)	0.26 (0.13)	0.17 (0.10)
Ndola	Background	0.20 (0.09)	0.21 (0.09)	0.21 (0.08)	0.23 (0.08)
	Population	0.531	0.542	0.556	0.571
	TROPOMI	0.13 (0.07)	0.13 (0.07)	0.17 (0.04)	0.10 (0.06)
Kitwe	Background	0.23 (0.09)	0.24 (0.08)	0.24 (0.08)	0.25 (0.08)
	Population	0.663	0.686	0.710	0.735

References

Beirle, S., Borger, C., Drner, S., Li, A., Hu, Z., Liu, F., . . . Wagner, T. (2019). Pinpointing nitrogen oxide emissions from space. *Science Advances*, *5*, eaax9800. doi: 10.1126/sciadv.aax9800

Dix, B., Francoeur, C., Li, M., Serrano-Calvo, R., Levelt, P. F., Veefkind, J. P., . . . de Gouw, J. (2022). Quantifying nox emissions from us oil and gas production regions using tropomi no2. *ACS EARTH AND SPACE CHEMISTRY*, *6*(2), 403-414. doi: 10.1021/acsearthspacechem.1c00387